Brain Research Unit
O.V. Lounasmaa Laboratory
Aalto University School of Science
Espoo, Finland
and
Neuroscience Unit
Institute of Biomedicine/Physiology
University of Helsinki
Helsinki, Finland

Functional and anatomical brain networks

Brain networks during naturalistic auditory stimuli, tactile stimuli and rest. Functional network plasticity in early-blind subjects.

Robert Boldt

ACADEMIC DISSERTATION

To be presented, with the permission of the Faculty of Medicine of the University of Helsinki, for public examination in Lecture hall 2, Haartman Institute, on December 11th, 2014, at 12 noon.

Helsinki 2014

Supervised by:

Professor Synnöve Carlson,
Brain Research Unit
O. V. Lounasmaa Laboratory
Aalto University School of Science
Espoo, Finland
and
Neuroscience Unit
Institute of Biomedicine/Physiology
University of Helsinki
Helsinki, Finland

Reviewed by:

Assistant Professor Uri Hasson, Ph.D.
Department of Psychology
Princeton University, USA
Princeton, NJ, U.S.A

Docent Vesa Kiviniemi, M.D., Ph.D.
Oulu Functional Neuroimaging
Medical Research Center
University of Oulu and Oulu University Hospital
Oulu, Finland

Official opponent:

Professor and Director Tianzi Jiang, Ph.D.
Brainnetome Center and
National Laboratory of Pattern Recognition
Institute of Automation
The Chinese Academy of Sciences
Beijing, P. R. China

ISBN 978-951-51-0398-7 (Paperback)
ISBN 978-951-51-0399-4 (PDF)

Helsinki University Printing House
Helsinki 2014

Abstract

Hearing is a versatile sense allowing us, among other things, to avoid danger and engage in pleasurable discussions. The ease with which we follow a conversation in a noisy environment is astonishing. Study I in this thesis used functional magnetic resonance imaging to explore the large-scale organization of speech and non-speech sound processing during a naturalistic stimulus comprised of an audio drama. Two large-scale functional networks processed the audio drama; one processed only speech, the other processed both speech and non-speech sounds.

Hearing is essential for blind subjects. Anatomical and functional changes in the brains of blind people allow them to experience a detailed auditory world, compensating for the lack of vision. Therefore, comparing early-blind subjects' brains to those of sighted people during naturalistic stimuli reveals fundamental differences in brain organization. In Study II, naturalistic stimuli were employed to explore whether one of the most distinguishing traits of the auditory system—the left-lateralized responses to speech—changes following blindness. As expected, in sighted subjects, speech processing was left-hemisphere dominant. Curiously, the left-hemisphere dominance for speech was absent or even reversed in blind subjects.

In early-blind people, the senses beyond vision are strained as they try to compensate for the loss of sight; on the other hand, the occipital cortices are devoid of normal visual information flow. Interestingly, in blind people, senses other than vision recruit the occipital cortex. Additional to changes in the occipital cortex, the sensory cortices devoted to touch and hearing change. Data presented here suggested more inter-subject variability in auditory and parietal areas in blind subjects compared with sighted subjects. The study suggested that the greater the inter-subject variability of the network, the greater the experience-dependent plasticity of that network.

As the prefrontal areas display large inter-subject spatial variability, the activation of the prefrontal cortex varies greatly. The variable activation might partly explain why the top-down influences of the prefrontal cortex on tactile discrimination are not well understood. In the fourth study, anatomical variability was assessed on an individual level, and transcranial magnetic stimulation was targeted at individually-chosen prefrontal locations indicated in tactile processing. Stimulation of one out of two prefrontal cortex locations impaired the subjects' ability to distinguish a single tactile pulse from paired pulses. Thus, the study suggested that tactile information is regulated by functionally specialized prefrontal subareas.

Contents

List of original publications

This thesis is based on the following publications:

I. **Boldt, R**, Malinen, S, Seppä, M, Tikka, P, Savolainen, P, Hari, R, Carlson, S: Listening to an audio drama activates two processing networks, one for all sounds, another exclusively for speech. PLoS One, 2013; 8(5):e64489.

II. **Boldt R**, Carlson S: Left-hemisphere dominance for naturalistic speech in sighted subjects—lateralization absent in early-blind subjects. Submitted.

III. **Boldt, R**, Seppä, M, Malinen, S, Tikka, P, Hari, R, Carlson, S: Spatial variability of functional brain networks in early-blind and sighted subjects. Neuroimage 2014; 95:208–216.

IV. *Gogulski J, ***Boldt R**, Savolainen P, Guzmán-López J, Carlson S, Pertovaara A. A segregated neural pathway for prefrontal top-down control of tactile discrimination. Cerebral Cortex, 2013, Aug 19 [Epub ahead of print]

*Shared first authorship

The publications are referred to in the text by their roman numerals.

Contributions of the author

I was the principal author of studies I-III. I contributed to the measurements, data analysis, and writing of Study IV. I also participated in the planning of Study IV, but not from the start. My coauthors provided assistance at all stages in all studies.

Abbreviations

AUC	area under the curve
BOLD	Blood-oxygen-level-dependent
DTI	diffusion tensor imaging
EPI	echo-planar imaging
fMRI	functional magnetic resonance imaging
FNC	functional network connectivity
FWE	family-wise error corrected
hs	hotspot
IC	independent component
ICA	independent component analysis
ISC	inter-subject correlation
MFG	middle frontal gyrus
MNI	Montreal Neurological Institute (MNI) coordinate system
MRI	magnetic resonance imaging
PFC	prefrontal cortex
ROC	receiver operating characteristics
ROI	region of interest
S1	primary sensory cortex
SFG	superior frontal gyrus
TE	echo time
TMS	transcranial magnetic stimulation
TR	repetition time

1. **Introduction**

In a utopian (or dystopian) not-too-distant future, brain activity is measured while subjects freely interact with the environment. For now, naturalistic settings during brain scanning are best mimicked when subjects engage in conversation (Stephens et al., 2010), play games (Kätsyri et al., 2013; Montague et al., 2002), or view movies (Hasson et al., 2004; Lankinen et al., 2014). The first brain-scanning experiments employing naturalistic stimuli explored inter-subject similarities of brain activity in subjects viewing a movie (Bartels & Zeki, 2004; Hasson et al., 2004). Thereafter, researchers employed naturalistic stimuli to gather information about how senses, such as hearing, function (Wilson et al., 2008). Since hearing helps us to shift our attention to a potentially harmful stimulus, avoid danger, and communicate, hearing is arguably our most important sense. One of the marvelous traits of our auditory system is how it manages to segregate speech from other sounds continuously surrounding us. Study I in this thesis explored the large-scale organization of speech and non-speech sound processing during a naturalistic stimulus derived from an audio drama.

Naturally, people with impaired vision are very dependent on hearing. Anatomical and functional changes in the brains of blind people reflect the coping strategies adopted by blind people to manage life in the dark. Therefore, comparing early-blind subjects' brains to those of sighted people during naturalistic stimuli can reveal instructive differences in brain organization. Accordingly, earlier studies suggest that listening to speech activates the right hemisphere more in blind than in sighted subjects (Röder et al., 2000; Röder et al., 2002). In Study II, naturalistic stimuli were employed to explore whether one of the most distinguishing traits of the auditory system—the mostly left-lateralized responses to speech—changes following blindness.

In early-blind people, the senses beyond vision are strained as they try to compensate for the loss of sight; on the other hand, the occipital cortices are devoid of normal visual information flow. Interestingly, in blind people, senses other than vision recruit the occipital cortex (Bavelier & Neville, 2002; Pascual-Leone et al., 2005). Additionally, the sensory cortices devoted to touch (Sterr et al., 1998) and hearing (Elbert et al., 2002) expand. In fact, the areas responding to sound in blind people are described as an "extended network". This extended network seems to react less strongly to sounds than the auditory areas of sighted subjects (Gougoux et al., 2009; Watkins et al., 2013).

The wiring of brain networks is both congenitally determined (Glahn et al., 2010; Jamadar et al., 2013) and shaped by experience (Jang et al., 2011; Thompson et al., 2001). The brain networks of infants are quite similar (Fransson et al., 2007), but inter-subject differences accumulate with age (Fair et al., 2009; Satterthwaite et al., 2013). Thus, it is credible that compensatory changes following sensory loss affects the brain networks uniquely in each subject (Lee et al., 2012). We hypothesized that the more experience-dependent plasticity a brain network undergoes following sensory loss, the more the brain network extent is expected to vary between subjects. This hypothesis was explicitly tested in Study III by assessing the variability of auditory, occipital and other functional networks in blind and sighted subjects.

Variability of anatomical and functional connectivity increases noise in group measurements (Speelman & McGann, 2013). The large inter-subject variability of frontal areas (Mueller et al., 2013) could be one of the reasons why it is hard to segment the prefrontal cortex (PFC) into functional subareas. In Study IV, diffusion tensor imaging (DTI) and tractography were employed to search for individual anatomical tracts connecting the primary sensory cortices to prefrontal areas. We then hypothesized that prefrontal areas modulate tactile perception by top-down mechanisms. We stimulated individually-chosen prefrontal primary somatosensory tracts with transcranial magnetic stimulation (TMS) while subjects performed a tactile discrimination task. Our aim was to find out whether we could influence tactile processing by TMS-induced top-down modulation of the primary sensory cortex.

2. Literature review

2.1 The auditory system

2.1.1 Anatomy and physiology of the auditory system

Hearing is the process of translating sound into a meaningful auditory signal. Figure 1 shows the structures that convey sound waves to the auditory cortex. Changes in air pressure (sounds) push the eardrum, a thin membrane at the transition between the outer and middle ear. Three small bones, together called the ossicles are located in the air-filled middle ear and convey the vibrations of the eardrum to the inner ear's oval window. The vibrations of the oval window are transferred to the fluid located in the spirally-formed cochlea (Hudspeth, 1989). The ossicles amplify the movement of the eardrum twentyfold. This amplification is important since the resistance to movement is larger in the fluid-filled cochlea compared with that of the air-filled middle ear. The pressure applied at the oval window moves the round window at the other end of the cochlea. The cochlea of the inner ear contains a tonotopically organized basilar membrane. The movement of the oval window produces vibratory movements in the basilar membrane. Since the basilar membrane is narrow and stiff at the base but wide and floppy at the apex, low-frequency vibrations move the apex, while high frequencies move the base of the basilar membrane (Bear et al., 2001). Motion of the basilar membrane causes movement of hair cells in the organ of Corti, contained in proximity to the basilar membrane. Bending of cilia, at the top of the hair cells, results in the release of neurotransmitters that in turn gives rise to an action potential propagating along the auditory nerve. The resulting action potential encodes the auditory signal's frequency, intensity and time-course (Hudspeth, 1989). The action potentials move along the auditory nerve to the ventral cochlear nucleus and the superior olive of the brainstem. From here, the signal continues to the inferior colliculus, medial geniculate nucleus of the thalamus and finally to the primary auditory cortex (Hudspeth, 1997). The primary auditory cortex, comprising parts of the superior temporal gyrus and Heschl's gyrus (Morosan et al., 2001), is tonotopically organized (Merzenich & Brugge, 1973; Moerel et al., 2012). Additionally, some neurons are intensity-tuned (Bear et al., 2001). Both hemispheres receive input from both ears; thus, in the case of unilateral cortical lesion, auditory functions are preserved (Bear et al., 2001).

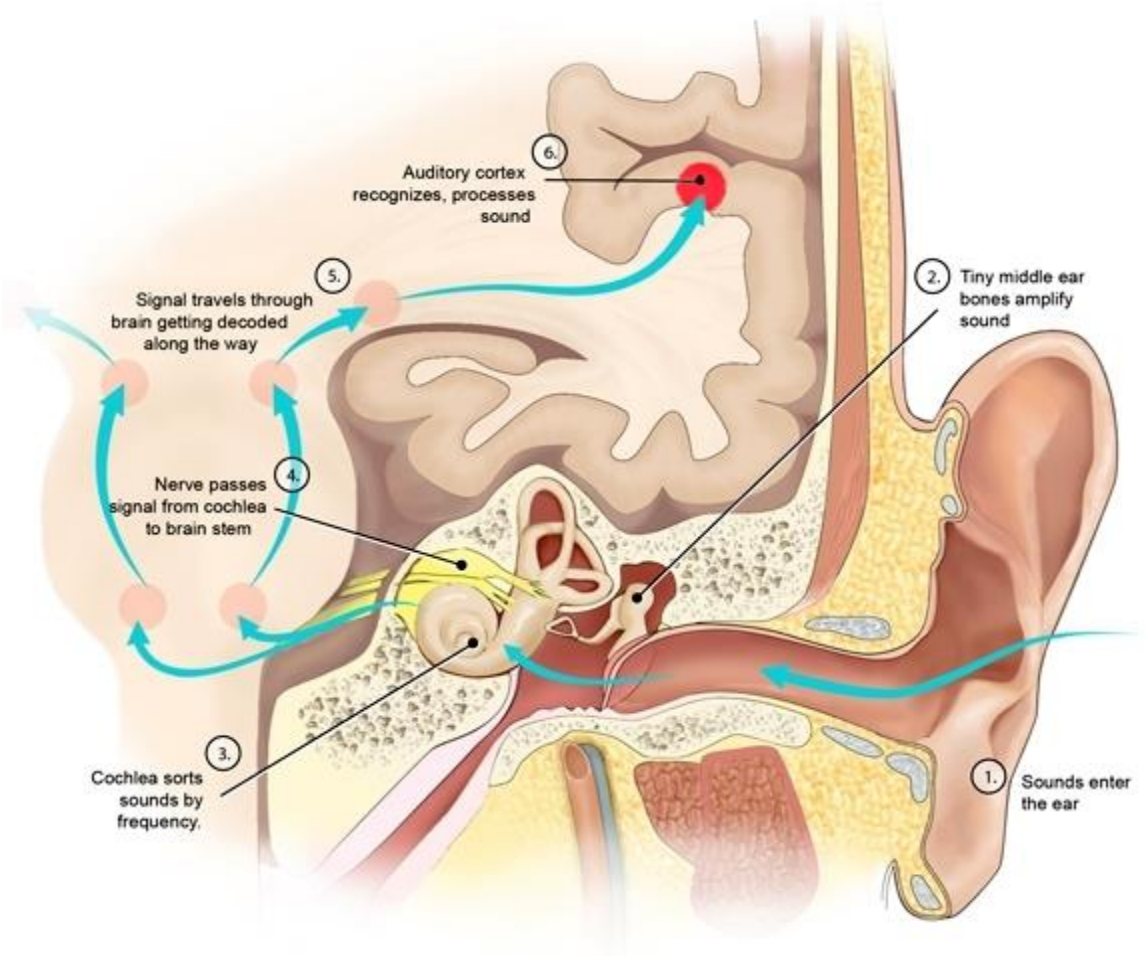

Figure 1 *Anatomy of hearing. First, sound waves enter the outer ear. The eardrum in the middle ear transforms the sound waves into vibrations that are amplified by the ossicles. The cochlea of the inner ear transforms the signal into action potentials that are conveyed by the auditory nerve to the brainstem, thalamus, and finally to the primary auditory cortex. Source Wikimedia Commons. Credit: Zina Deretsky, National Science Foundation.*

2.1.2 Speech and non-speech sound perception

Papua-New Guinea strikingly emphasizes how naturally languages evolve for humans. In Papua-New Guinea, a population of 3.9 million people speak 832 languages—that is, on average, one language for every 4500 people (Anderson, 2004). Apparently, language is so innate to humans that a speechless tribe has yet to be found (Bear et al., 2001)!

Studies of speech impairments resulted in the functional specialization hypothesis, suggesting specialization of brain areas for specific tasks. Franz Joseph Gall was one of the first to suggest that lesions to specific areas of the brain cause selective speech impairments. Therefore, he reasoned, some brain areas must be specifically used for speech (Bear et al., 2001). During the 19th century, Paul Broca and Carl Wernicke provided further evidence that different brain areas had different roles in speech

production and language processing. Broca studied several aphasic subjects with left-sided frontal lobe lesions and reasoned that the left hemisphere controls language. Carl Wernicke described deficits in speech processing after lesions to the left posterior superior temporal gyrus and suggested that this area is responsible for giving speech a meaning while Broca's area controls speech production. Extending the findings of Wernicke, Norman Geshwind proposed a theory of language processing and production, called the Wernicke-Geschwind model (Bear et al., 2001; Geschwind, 1970). According to the model, describing the process of mimicking a word, a word is first processed in the auditory cortex. Meaning to the word is then supplied in Wernicke's area and the angular gyrus. From there, the neural signal representing the word proceeds through the arcuate fasciculus to Broca's area where 'the word' is transformed to the muscular movements required for speech production. The motor cortex is responsible for coordinating the movements of the articulate organs to produce speech. The Wernicke-Geschwind model is—according to current science—outdated, but the longevity of the model is striking evidence of its explanatory power (Poeppel et al., 2012).

A recent dual stream model explaining speech perception proposes that speech processing follows a ventral stream for speech comprehension and a dorsal stream for controlling articulation (Hickok & Poeppel, 2007). Both streams start with a spectro-temporal analysis carried out bilaterally in the supratemporal cortex. The ventral stream involves the temporal lobes, the middle temporal gyrus (MTG) and the inferior temporal sulcus, while the dorsal stream encompasses parietal and frontal areas along with Broca's area. According to the dual stream model, the parietal-temporal boundary works as a hub for input from other modalities and sensorimotor integration. The dorsal stream is thought to be very left-lateralized while the ventral stream is weakly left-lateralized (Hickok & Poeppel, 2007).

The motor theory of speech suggests the involvement of motor networks in both speech comprehension and perception. The theory proposes that speech is perceived rather as corresponding vocal tract gestures than as sound patterns (Liberman & Mattingly, 1985). As speech comprehension probably includes several specialized streams integrating large portions of the cortex (Poeppel et al., 2012), one theory of speech perception does not necessarily exclude other theories. Importantly, speech comprehension benefits from distributed connectivity (Obleser et al., 2007), and even perceiving meaning to words and sentences probably involves a distributed network (Poeppel et al., 2012). Several temporal processing windows are involved during naturalistic listening and speech processing (Stephens et al., 2013). Low-level areas process speech on a timescale of seconds, whereas higher brain areas, such as the parietal and frontal areas, integrate information needed to understand a full narrative (Lerner et al., 2011).

The temporal information conveyed by speech is important for speech comprehension. Naturalistic speech perception probably relies on continuous chunking of speech into ~200-ms frames. Thus, speech perception is probably dependent on syllable flow, since syllable duration is approximately in this range (Luo & Poeppel, 2007). Speech comprehension is not only a bottom-up process but relies equally on top-down control. For instance, predictable words are easier to understand than unexpected words (Schwanenflugel & Shoben, 1985). In fact, in some brain areas, the speaker's brain

activation is preceded by the listener's brain activation (Stephens et al., 2010). The better the anticipatory coupling of the speaker-listener, the better the understanding is (Stephens et al., 2010).

Language and handedness are both often lateralized to the left. The left-hemisphere dominance for speech, suggested first by Paul Broca, is supported by studies using the invasive Wada procedure to show that in 96% of right-handed subjects, speech is represented in the left hemisphere. In contrast, only 70% of the left-handed have speech represented in the left hemisphere (Rasmussen & Milner, 1977). The Wada procedure requires an injection of barbiturate to one hemisphere at a time through the internal carotid artery and is thus invasive. Functional magnetic resonance imaging (fMRI) might be an equally reliable but non-invasive alternative to the Wada procedure for studying hemispheric language representation (Binder et al., 1996; Dym et al., 2011). The gross anatomy of the brain mirrors the hemispheric differences: the left planum temporal, which is involved in language processing, is bigger than the right (Geschwind & Levitsky, 1968). Interestingly, hemispheric asymmetry is already present in infants' brains and could thus be congenital (Witelson & Pallie, 1973). Genetic models are, however, insufficient to explain why speech is left-lateralized, so experience-driven plasticity could partly contribute to the development of left-dominant responses to speech (Günter, 2006).

Music perception involves parts of the speech processing network (Koelsch, 2011; Koelsch et al., 2002). Although speech and music perception might activate the same regions, it seems that the brain responses to music are more right-lateralized than responses to speech (Tervaniemi & Hugdahl, 2003). The same goes for recognizing voices, which mainly activate a right hemispheric network (Formisano et al., 2008). The differences in lateralization between speech and music might be due to different temporal and spectral characteristics and demands contained in speech compared with music (Koelsch, 2011). During naturalistic stimuli, the brain processes non-speech sounds differently and in distinct areas from speech sound processing (Lahnakoski et al., 2012). As presented above for speech processing, a dual-pathway model has also been proposed for non-speech sound processing in both humans and animals. According to the model, the ventral stream processes object identification and the dorsal stream processes localization of sounds in space (Lewis et al., 2004; Rauschecker, 2011; Romanski et al., 1999). It is unclear if speech and non-speech sound processing conform to these streams (Rauschecker, 2011).

2.2 Anatomy and physiology of the somatosensory system

Although we traditionally refer to touch as one sense, it is comprised of at least four different modalities: proprioceptive, thermal, pain, and tactile somatic sensation (Tortora & Derrickson, 2009). The skin contains many types of receptors reacting to these different aspects of touch. The most prevalent touch receptors are mechanoreceptors that react to physical distortion of the skin, resulting in action potentials that spread through the primary afferent axons to the dorsal root ganglion of the spinal cord or brain stem. The dorsal column-medial lemniscus pathway conducts the sensation of touch, pressure,

vibration and conscious proprioception to the brain (Tortora & Derrickson, 2009). This pathway leads from the entry point in the spinal cord along the dorsal column to the dorsal column nuclei in the medulla. The medulla is the termination point of the first-order neuron that started at the mechanoreceptor. Here, the neuron synapses with the second-order neuron that then crosses the midline. The second-order neuron then continues through the medulla, pons, and midbrain, and synapses with the third-order neuron in the ventral posterior nucleus of the thalamus, which is the end point of the second-order neuron. From here onwards, the thalamic third-order neuron projects to the primary somatosensory cortex positioned in the central sulcus and the postcentral gyrus of the parietal lobe. A lesion to the primary sensory cortex impairs somatic sensations (Bear et al., 2001).

The primary somatosensory cortex has a somatotopic arrangement with specific parts of the body represented in distinct areas. The size of the area representing the different parts of the body is proportional to the density, frequency of usage, and the importance of the sensory input received from the skin area. In the 1980s, the plasticity of the somatosensory cortex was addressed by surgically removing a finger of the owl monkey. Remapping of the cortex revealed that the area of the cortex initially devoted to the removed finger subsequently reacted to sensory stimulation of the adjacent fingers (Merzenich et al., 1984). With prolonged deprivation, the cortical remapping increased (Pons et al., 1991). Interestingly, to influence the cortical representation of the skin of a finger, it is enough to stimulate the finger more than the other fingers. Increased useage increase the fingers representation in the cortex (Elbert et al., 1995; Jenkins et al., 1990). Similarly, reorganization of the motor cortex happens surprisingly fast when subjects train for instance finger opposition sequences (Karni et al., 1995; Karni et al., 1998).

The encoding of complex tactile patterns, such as recognizing the keys in your pocket, requires large cortical receptive fields and likely involve the posterior parietal cortex. The Gerstmann syndrome reveals the importance of the posterior parietal cortex for more than just tactile perception. Gerstmann syndrome resulting in finger agnosia, writing disability, difficulty in learning or understanding arithmitic, and left-right disorientation, follows from a lesion to the inferior parietal lobule (Rusconi et al., 2010).

Perhaps the simplest test of tactile spatial resolution is the two-point discrimination threshold. Discrimination thresholds vary throughout the body, with the fingertips being the most sensitive parts. Since the fingertips have a disproportionally large representation in the cortex, much computational power is devoted to the fingertips. Perhaps this is the reason blind people read Braille with their fingertips rather than their elbow (Bear et al., 2001). Both spatial and temporal tactile discrimination tasks activate several cortical and subcortical areas. Functional magnetic resonance imaging reveals that the supplementary motor area and the anterior cingular gyri are activated bilaterally during tactile temporal discrimination (Pastor et al., 2004).

Tracing studies in non-human primates indicate that the primary sensory cortex has cortical connections with the PFC (Preuss & Goldman-Rakic, 1989), but the specific roles of these connections are unknown. However, it seems plausible that the PFC gates irrelevant information, thus aiding the performance of working memory tasks (Carlson et al., 1997; Hannula et al., 2010; Yamaguchi & Knight, 1990). Subjects with lesions in the

PFC perform poorly in working memory tasks including distractors (Chao & Knight, 1995).

2.3 Anatomy and physiology of the visual system

Vision not only transforms wavelengths of light to sensory perception, but allows us to deduct information from far-away scenes in the fastest possible way. When a photon enters the eye, it projects through the lens and the vitreous humor of the corpus to the retina. The retina consists of photoreceptor cells containing rods and cones. Rods provide night vision, whereas the three types of cones permit color vision since they react to different wavelengths of light. The photoreceptors are responsible for turning light into electrical signals, a process called phototransduction (Arshavsky et al., 2002). Photocell receptors synapse with bipolar cells that in turn project to ganglion cells conducting action potentials through the optic nerve to different parts of the brain (Bear et al., 2001).

The optic nerve conducts signals from the retina to the lateral geniculate nucleus in the thalamus through three different pathways: the parvocellular, magnocellular, and konicocellular pathways. Signals from the retina are also conducted to the superior colliculus of the midbrain, the basal optic system, and the pretectum. The superior colliculus and the basal optic system control eye movement. The pretectum controls the papillary size and circadian rhythm (Bear et al., 2001). Although still debated, brain tissue possibly responds directly to light. An fMRI experiment revealed changes in brain function when light was directed directly onto the brain through the ear canals (Starck et al., 2012).

From the thalamus, the optic radiation projects to the visual cortex in the occipital lobe. The visual cortex consists of a myriad of areas responsive to different parts of visual scenes. Orientation tuning emerges in the primary visual cortex (Hubel & Wiesel, 1959). The primary visual cortex also contains ocular dominance columns (Wiesel et al., 1974) and retinotopic maps (Daniel & Whitteridge, 1961). Occipital visual areas other than the primary and secondary visual cortex are referred to as extrastriate visual areas. These include visual areas V3, V4 and V5/MT which process various stimulus attributes. For instance, area MT reacts to moving stimuli (Zeki et al., 1991). Monkey studies suggest that at least 32 separate visual areas exist (Felleman & Van Essen, 1991). The receptive field sizes of the visual cortex seem to increase when moving from lower to higher visual areas (Nurminen, 2013).

A visual scene is usually rich in information. Thus, mechanisms guiding attention are necessary (Ungerleider & Leslie, 2000). The visual areas are arranged hierarchically, with increasingly complex information processed in areas positioned higher in the visual hierarchy. The dual stream hypothesis suggests that the dorsal and ventral stream project from the primary visual areas. The dorsal stream processes spatial attention; the ventral stream aids in recognition, identification and categorization of visual stimuli (Goodale & Milner, 1992; Milner & Goodale, 2008). The streams project to different parts of the brain, but interact with each other richly (Farivar, 2009). In addition to the occipital areas, frontal and parietal areas control visual attention (Ungerleider & Leslie, 2000).

In the visual system, genetic mechanisms as well as innate retinal firing shape the brain connections during fetal development (Goodman & Shatz, 1993). However, visual experience is necessary for the maintenance and full development of visual connections (Wiesel, 1982). An experiment involving newborn cats showed that, if one eyelid is sutured shut (monocular visual deprivation) for three months, the visual cortical cells became unresponsive to visual stimulation through the deprived eye. Most of the cortical cells normally responding to the deprived eye responded to visual stimulation of the non-deprived eye (Wiesel & Hubel, 1963). The non-deprived eye recruited the ipsilateral visual cortex at the expense of the deprived eye, and after a critical period, this change was permanent even after removing the sutures of the deprived eye. After suturation of both eyes (binocular visual deprivation) of a newborn cat for 3 months few active visual cortex cells, without tuned orientation preferences, remained (Hubel & Wiesel, 1963; Wiesel & Hubel, 1965a; Wiesel & Hubel, 1965b). Surprisingly, the cats with binocular visual deprivation had rather normal visual cortex structure, although cell shrinkage was prevalent; however, after the eyes were re-opened, the cats behaved as if blind. Wiesel and Hubel were awarded the Nobel Prize in 1981 for their discoveries concerning the plasticity of information processing in the visual system (Nobelprize.org).

2.4 Effects of early blindness on the brain

In all sensory systems, experience-driven synaptic plasticity is the last step of neuronal pathway formation and takes place mainly after birth. This experience-dependent refinement of the congenitally-wired brain is instrumental for the function of the human brain (Fagiolini & Hensch, 2000). After birth, all sensory systems are very sensitive to experience—this is the critical period. After this initial critical period, the brain remains plastic throughout life, but the sensitivity is decreased, and the mechanisms are different (Hensch, 2005).

As discussed in the previous chapter, cats with bilaterally sutured eyelids have rather normal structure of the visual cortex; however, although eyes are reopened after the deprivation period, the cats act as if blind. Considering that the visual cortex develops despite binocular visual deprivation, but is functionally inoperative, the ability of the nervous system to change following experience may be the basic mechanism that adapts us to our environment (Wiesel, 1982). The critical period refers to the time during which the brain retains its strong ability to rewire its neural connections into their final networks. It is thought that the critical period allows experiences to prune the neural networks, choosing the best neural connections available among several competing inputs (Hensch, 2005). The duration of the early critical period is specific for different brain areas but is quite limited in adulthood. However, after the critical period has ended, the brain remains plastic (Fagiolini & Hensch, 2000).

Both genetics (Brun et al., 2009; Glahn et al., 2010; Jamadar et al., 2013), practice (Jang et al., 2011) and disease (Greicius et al., 2004) influence the brain's function and structure. However, the effect of genes and environment on brain structure and function depends on the brain area, with strong genetic influences on sensory areas such as

occipital areas, and strong environmental effects on prefrontal areas (Brun et al., 2009). After damage to sensory organs, the central nervous system reorganizes as discussed previously. Learning new skills and extensive training also change the structure (Draganski et al., 2004; Maguire et al., 2000) and function (Herdener et al., 2010; Karni et al., 1995; Karni et al., 1998) of the brain.

In blind people, the somatosensory cortical area representing the Braille reading finger expands following reading practices (Pascual-Leone & Torres, 1993). Interestingly, disturbing the somatosensory system with TMS in blind subjects reading Braille does not result in more mistakes in Braille reading, while TMS to the occipital cortices of blind subjects does (Cohen et al., 1997). The occipital lobe usage in blind people during Braille reading is an example of cross-modal plasticity. Tactile sensations activate the primary visual cortex in early blind subjects. However, the critical period regulates this activation, and subjects who became blind after age 16 do not activate V1 during tactile discrimination tasks (Sadato et al., 2002).

In addition to cross-modal plasticity, intra-modal plasticity is present following early blindness. Subjects reading Braille with three fingers and at least some subjects who read Braille with one finger exhibit disorganization of the normal pattern of finger representation in the primary sensory cortex (Sterr et al., 1998). Furthermore, the subjects who use three fingers to read Braille misidentify the fingers following a brief touch to the fingers more often than do sighted control subjects, indicating smearing of the representation areas of the fingers in the blind (Sterr et al., 1998).

Cross-modal plasticity had intrigued people since the 17th century, when Molyneux proposed the following thought-experiment:

> "Suppose a man born blind, and now adult, and taught by his touch to distinguish between a cube and a sphere of the same metal, and nighly of the same bigness, so as to tell, when he felt one and the other, which is the cube, which the sphere. Suppose then the cube and sphere placed on a table, and the blind man be made to see: quaere, whether by his sight, before he touched them, he could now distinguish and tell which is the globe, which the cube?"
>
> *-Question by William Molyneux to John Locke (Locke, 1700)*

Molyneux and Locke were of the opinion that a cross-modal transformation of noumenal information derived with the sense of touch to the visual sense is impossible. On the other hand, we know that the entire cortex is highly interconnected. Pascual-Leone et al. (2005) suggested two types of plasticity, in the brains of blind people: compensatory plasticity or general loss. These two broad types of plasticity either aid the blind subject and are compensatory, or lead to maladjustments as e.g. the inability to tell fingers apart (Sterr et al., 1998) or impairing localization of certain sounds (Gori et al., 2014; Zwiers et al., 2001). Functional connectivity studies in blind people show evidence for both the general loss hypothesis and compensatory plasticity. For instance, connectivity within the occipital cortex is reduced, whereas connectivity between language regions, frontoparietal regions and the occipital cortex are strengthened (Liu et al., 2007; Wang et al., 2014). Furthermore, blind people display superior verbal memory compared with the sighted,

possibly explained by the recruitment of primary visual areas during verbal memory tasks (Amedi et al., 2003). Today, we now know the answer to Molyneux's problem: if vision is restored with modern surgical methods after years of blindness, subjects will not (at least quickly) learn to visually recognize objects introduced to them by touch (Held et al., 2011).

Countless figures of speech that stir from visual perception demonstrate that vision influences our spoken language.

> "Love is a smoke raised with the fume of sighs."
>
> *-Romeo and Juliet. Act I. Scene I. William Shakespeare*

Such grasping figures of speech makes you assume that speech networks are affected by vision. Figures of speech such as idioms (Rapp et al., 2012) and metaphors (Bohrn et al., 2012) activate a left-lateralized network. Naturally, the influence of vision on speech networks would be absent in blind subjects.

2.5 Functional magnetic resonance imaging

Atoms are the building blocks of matter. Atomic nuclei are defined by their spin and magnetic moment. Spin and magnetic moment can only possess discretely distributed values. Thus, magnetic fields affect atomic nuclei in a predictable manner. A magnetic resonance imaging (MRI) scanner utilizes the magnetic properties of the hydrogen ions of water to construct a high-resolution image of an object of interest. The MRI machine consists of: (i) a continuous static longitudinal magnetic field; (ii) an intermittent resonating magnetic field delivering radio frequency pulses; and (iii) gradient coils used for spatial encoding of the proton positions. If the resonating magnetic field sends radio frequency pulses at a particular frequency (the resonance frequency), it excites the hydrogen ions of water. When the radio frequency pulse is turned off, several signals can be detected from the hydrogen ions (Huettel et al., 2004). The measurable signals discussed here are: (i) the T1 recovery, (ii) the T2 decay, and (iii) the T2* decay.

Wolfgang Pauli suggested in the 1920s that atomic nuclei have magnetic properties that could be manipulated experimentally (Huettel et al., 2004). Isidor Rabi received the Nobel prize in physics in 1944 for demonstrating magnetic resonance effects in lithium atoms (Nobelprize.org). Felix Bloch and Edward Purcell shared the Nobel price in 1952 for independent discoveries of magnetic resonance in solid materials (Nobelprize.org). In 1971, Raymond Damadian distinguished cancerous tissue from healthy tissue with magnetic resonance effects (Damadian, 1971); the experiment fueled an increased interest in MRI of biological tissues. Paul Lauterbur reported the first magnetic resonance images of a pair of water-filled tubes sitting in a bath of heavy water in 1973 (Lauterbur, 1973). Echo-planar imaging (EPI), introduced by Peter Mansfield in 1976, reduced the time needed to collect an image by introducing gradient fields (Mansfield, 1977; Mansfield & Maudsley, 1976). Raymond Damadian created the first human MRI-scanner in 1977.

Lauterbur and Mansfield shared the Nobel prize in physiology and medicine in 2003 (Nobelprize.org). In the 1990s, Seiji Ogawa and colleagues discovered the blood-oxygen-level-dependent (BOLD) effect, which is now widely used to study brain function (Ogawa et al., 1990; Ogawa et al., 1992).

The majority of the human body consists of water. In a static longitudinal magnetic field, the spin axis of the water protons aligns with the direction of the longitudinal field. If, however, the spin axis is tipped away from the longitudinal direction, it starts to precess at the Larmor frequency, a rate that is proportional to the strength of the main magnetic field. The spin axis can be tipped by a radio frequency pulse oscillating at the resonance frequency of hydrogen protons (~128 Hz at 3T). The radio frequency pulse flips the net magnetization vector of the protons into the transverse plane, and the protons start spinning in phase. The flip angle describes the number of degrees the spin axis of the protons is tipped from the main magnetic field. When the resonating magnetic field is turned off, the protons start to realign to the static field. T1 recovery describes the realignment of the net magnetization vector to the initial equilibrium state. The T1 recovery can be measured as a change in the protons' net magnetization, leading to a change of magnetic flux, which sensors can measure as a change in voltage. Protons of different tissues take a different amount of time to return to the static magnetic field, thus leading to T1 contrast. The T1 signal is suitable for measuring contrast between tissues, such as the grey and white matter (Huettel et al., 2004). At 3 tesla grey and white matter have T1 values of 1331 and 832 ms, respectively (Wansapura et al., 1999).

When the radiofrequency pulse is turned off, the excited protons return to an equilibrium state. Meanwhile, the net movement in the transverse plane becomes less coherent and, thus, the transverse net magnetization will decay over time. This is the basis for the T2 decay, the time constant measuring loss of coherence (accumulated phase difference) in the transverse plane. Both the T1 and T2 relaxation times can be described by the Bloch equations, characterizing the change in longitudinal and transverse magnetization over time (Bloch, 1946; Huettel et al., 2004).

For functional brain imaging, fast collection of brain images can be achieved by echo-planar imaging. When performing EPI, each radio frequency pulse is followed by gradient echoes providing spatial encoding. As the static magnetic field is shifted with gradients, different image orientations are obtained. It is the gradient coils that make noise during MRI imaging. The gradient coils allow several slices to be imaged during one repetition of the oscillating magnetic field (Huettel et al., 2004). Thus, the gain in imaging speed is achieved by selectively exciting layers of spins (Mansfield, 1977). Using EPI and 3-mm voxels, a scanner can sample a whole brain in 2–3 seconds, which is fast enough for BOLD imaging (see next paragraph). If, however, one would like to explore MRI contrast mechanisms measuring direct neuronal activation, faster imaging is compulsory. Dynamic inverse imaging can achieve temporal resolution in the range of milliseconds by deriving spatial information from detectors rather than encoding the spatial location with gradients such as in EPI (Lin et al., 2006).

Since brain cells have little energy storage capacity, blood must continuously supply glucose and oxygen to them. Although the mechanisms underlying this delivery are not completely understood, areas with increased neuronal activity receive increased amounts

of oxygenated blood flow and volume. Thus, increased rather than decreased amounts of oxygenated blood in a local brain area seems to indicate neuronal activity within that area (Huettel et al., 2004). Blood contains hemoglobin that has two different magnetic states. Fully oxygenated hemoglobin is diamagnetic, so it has zero magnetic moment. However, deoxygenated hemoglobin is paramagnetic and, thus, it distorts the magnetic field and introduces inhomogeneous T2* decay in areas where oxygen is sparse. Therefore, the signal in the transverse plane becomes less coherent (decays faster) in areas where large quantities of deoxygenated hemoglobin is present. Thus, the BOLD signal originates from the different magnetic properties of oxygenated and deoxygenated hemoglobin and is the basis of fMRI. Since fMRI measures changes in blood volume and flow, the fMRI signal is indirectly correlated to neural activity (Logothetis, 2003; Logothetis et al., 2001). The theoretical spatial resolution of fMRI is very good, ~1 mm, but the temporal resolution is in the range of seconds owing to the slow hemodynamic response (Logothetis, 2008). The hemodynamic response function models the shape of the hemodynamic response as measured by fMRI (Friston et al., 1994). The hemodynamic response function is often used in block and event-related design to transform the stimulus regressor into a shape theoretically resembling the hemodynamic response.

2.5.1 Functionally connected networks

The functional specialization theory, proposing a relationship between brain function and location, was first suggested by Franz Joseph Gall and Johann Gaspar Spurzheim in the 19th century (Bear et al., 2001). The functional specialization theory was supported by case studies of patients such as Phineas Gage whose behavior was altered by brain lesions (Damasio et al., 1994). Since the early 20th century, Brodmann and others proposed that the brain is divided into subregions (Bear et al., 2001). The Brodmann areas are one of the earliest examples of histological divisions in the brain (Brodmann, 2007; Zilles & Amunts, 2010). However, the division of the brain based on the Brodmann areas corresponds at times poorly with specific functions. Perhaps the biggest drawback of the early cytoarchitectonic maps was that they were not registered to a stereotactic standard space and did not take individual variations into account (Toga et al., 2006; Zilles & Amunts, 2010). However, cytological maps are important when studying brain areas, as the demarcation of brain areas cannot be inferred based on macroscopic brain anatomy alone (Toga et al., 2006; Tomaiuolo et al., 1999; Zilles et al., 1997).

Functionally connected networks are comprised of temporally-correlated regions and were first shown using fMRI in the bilateral motor cortices (Biswal et al., 1995). Functionally connected regions are apparent even in the resting brain; such networks are called resting-state networks (Deco et al., 2011). Some of the most consistent resting-state networks are: the default-mode network, the sensorimotor network comprising the pre- and post-central gyri, some vision-related networks and a superior temporal gyrus network comprising auditory areas (Damoiseaux et al., 2006). The default-mode network is inactivated during task performance and might be related to innate processes (Raichle et

al., 2001). The functional significance of the default-mode network is still debated, but activity in this network has been related to e.g. mind wandering (Christoff et al., 2009) and introspection (Raichle et al., 2001). The connectivity of at least the default-mode network persists despite light sedation of subjects (Greicius et al., 2008).

A currently popular analysis method for estimating functionally connected networks is independent component analysis (ICA) which decomposes brain activity into maximally spatially independent networks (Calhoun & Adali, 2006; Calhoun & Adali, 2012; Calhoun et al., 2001; Kiviniemi et al., 2003). ICA has many advantages over seed-based correlation methods as it reliably reveals comparable resting-state and task networks, despite coactivation of distinct networks during tasks (Di et al., 2013; Smith et al., 2009). Measuring distributed connections by investigating connectivity between ICA-derived functional networks is a promising tool for studying whole-brain connectivity (Abou-Elseoud et al., 2010; Allen et al., 2014; Jafri et al., 2008; McKeown et al., 1998; McKeown et al., 1997; McKeown & Sejnowski, 1998).

Many brain areas show considerable inter-subject differences, limiting the accuracy of functional localization (Brett et al., 2002). However, functional connectivity studies can also address the inter-subject variability of brain areas. Voxelwise whole-brain analyzes reveal that the inter-subject variance is largest in brain areas that have expanded the most during evolution, such as frontal and parietal association areas (Mueller et al., 2013). As sensory and motor networks are mainly rearranged during childhood, while association areas rearrange throughout adulthood (Littow et al., 2010), experience-dependent changes could explain why the association areas of adults show larger inter-subject differences than sensory networks.

2.5.2 Naturalistic stimuli during fMRI recordings

Uri Hasson pioneered the use of naturalistic stimuli during fMRI recordings (Hasson et al., 2004). Naturalistic stimuli have also been combined with imaging modalities such as electroencephalography (Whittingstall et al., 2010) and magnetoencephalography (Lankinen et al., 2014). Inter-subject correlation (ISC) is one of the successful techniques used for examining brain responses to naturalistic stimuli (Brennan et al., 2012; Hasson et al., 2004; Nummenmaa et al., 2012; Wilson et al., 2008). It is especially suitable for complex stimuli as it neither requires an assumption about which parts of the stimulus are processed by the brain nor in which area the brain processes the stimulus. ICA is also a useful tool for analyzing brain imaging data collected during presentation of naturalistic stimuli since it can subdivide the brain into functionally coherent networks (Malinen & Hari, 2011; Malinen et al., 2007). Studies using naturalistic stimuli can also help to validate findings based on simple stimuli (Rust & Movshon, 2005). Additionally, rich naturalistic stimuli activates more brain areas than simple stimuli (Bartels & Zeki, 2005). It is also more pleasant for a subject to attend to e.g. an audio drama than to listen to beeps or tones.

2.6 Diffusion weighted magnetic resonance imaging

Brownian motion, the basis of DTI, was first described 60 BC by the Roman poet Lucretius (99 BC–55 BC), but was named after botanist Robert Brown (1773–1858) (Tóthová et al., 2011). In one of the Annus Mirabilis papers, Albert Einstein proposed that a macroscopic structure can move in a random fashion under the influence of the thermal motion of molecules (Einstein, 1905). The distance moved by a particle in pure liquid is proportional to the thermal energy of the molecules and is randomly distributed if molecules are not hindered by any structures; such movement is called isotropic. In brain tissue, however, the diffusion of water molecules is hindered by various structures such as cell membranes and fibers, and the diffusion is anisotropic. Diffusion weighted MRI is based on the effect Brownian movement of water molecules exerts on the T2 signal. If the MRI scanner employs a gradient pulse intended to rephase the spins, the gradient pulse is unsuccessful in rephasing protons that have moved by diffusion. Thus, the signal decay is related to the amount of diffusion. Since the magnetization changes if diffusion is present, the Bloch equations discussed in the fMRI section must be coupled with diffusion tensor vectors (Torrey, 1956). These equations are called the Bloch-Torrey equations. If many diffusion directions are estimated, an image of the likelihood of different diffusion directions emerges (Jones, 2010).

The first paper on diffusion imaging was fueled by a desire to understand better the anatomy of the human brain (Basser et al., 1994a; Basser et al., 1994b). DTI tract maps coincide with earlier invasive work (Catani et al., 2002; Lawes et al., 2008). Diffusion imaging reveals anatomical connectivity, whereas fMRI reveals functional connectivity. It is useful to look at both anatomical and functional connectivity since they are predictive of each other but also reveal unique connections (Greicius et al., 2009; Honey et al., 2009).

2.7 Transcranial magnetic stimulation

Arsenne d'Arsonval conducted the first known TMS experiment in 1896 by placing the subject's head inside a coil with a pulsating 42 Hz field (Cowey, 2005). TMS is a noninvasive way to excite the brain and has gained widespread use and interest (Hallett, 2000). When using single pulse TMS, the coil is placed on the scalp and a brief electrical current is passed through the coil. The current gives rise to a brief, strong magnetic field that penetrates the skin and the skull and induces, through electromagnetic induction, an electromotive force in the brain tissue underneath the coil. According to the Maxwell-Faraday equations, the magnetic field produces a change in the electrical potential across the cell membrane of the neurons in the targeted areas. This can produce either hyperpolarization or depolarization of the neurons. A single TMS pulse usually causes depolarization of the neural cell membrane, which in turn results in an action potential (Wasserman, 2007).

Many different TMS pulse sequences exist, ranging from single pulse TMS to repetitive TMS. In a monophasic pulse the current travels in one direction, while in a biphasic pulse the current reverses, traveling through the coil in both directions. Biphasic

stimulation produces more powerful motor evoked potentials than monophasic stimulation. Repetitive TMS causes frequency-dependent effects on e.g. motor excitability and inhibition. Low-frequency stimulation causes a transient reduction in motor evoked potentials; high-frequency stimulation increases motor evoked potentials and reduces cortical inhibition (Fitzgerald et al., 2006). Repetitive TMS can also cause prolonged effects (Lefaucheur, 2009) and can be used for testing subjects after the TMS stimulation. However, a single monophasic stimulation pulse provides spatially more restricted stimulation than biphasic stimulation (Hannula et al., 2010), and temporally more restricted stimulation than repetitive stimulation. High-frequency repetitive TMS might induce epileptic seizures in susceptible patients, but otherwise TMS is considered safe. Possible clinical uses for TMS includes determining the hemisphere dominance for language in patients previous to brain surgery (Hallett, 2000; Wasserman, 2007)

TMS has some major advantages over fMRI. While fMRI shows the brain areas that are involved with the experimental task, TMS can transiently introduce a virtual lesion and interfere with the task (Cowey, 2005). Thus, TMS can be used to infer whether a particular area is causally involved with the performance of a task (Bona et al., 2014). Combining TMS with MRI measurements such as fMRI and DTI has many beneficial applications. Combining the TMS coil with an optical tracking system and MR images of the subject, as seen in Figure 2, allows exact targeting of brain areas. The resolution of TMS can be as good as 8−13 mm (Hannula et al., 2005). As the monophasic pulse duration is only ~1 ms, the trigger system usually imposes the temporal limit of TMS experiments. Thus, TMS allows reasonable spatial resolution and excellent temporal resolution.

Diffusion weighted images and tractography can enable stimulation of specific nerve bundles at an individual level, and improve the spatial specificity and efficacy of TMS (Nummenmaa et al., 2014). Moreover, TMS-DTI experiments can be used to explore the functions of areas with large inter-subject spatial variability, such as the PFC (Hannula et al., 2010; Savolainen et al., 2011).

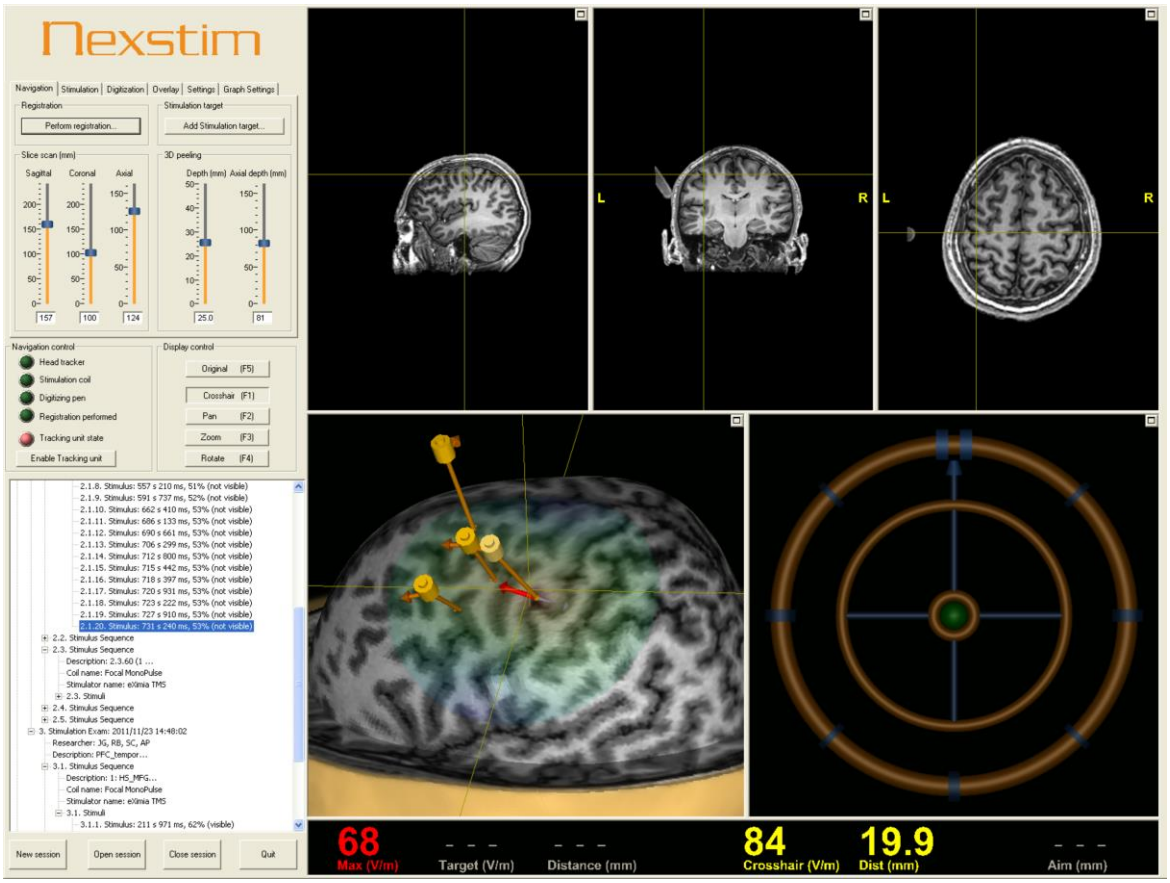

Figure 2 *Screenshot of the Nexstim TMS computer interface. Optical tracking of the subject's head combined with a 3D model of the head constructed from the subject's structural MR images allows the TMS pulses to be targeted at specific brain areas. The TMS targets are saved; thus, one can repeat stimulation of targets used in an earlier session. The circle pictured in the right bottom corner provides information about the current coil position and orientation compared with a repeated target. The red arrows indicate the direction of the current.*

3. Aims of the thesis

Of the four publications included in this thesis, two explored the processing of a naturalistic auditory stimulus (I and II). Two of the publications addressed functional and anatomical connectivity at an individual level (III and IV). Studies I and IV included only neurotypical subjects; studies II and III compared neurotypical and early-blind subjects.

The overall goal was to investigate functional and anatomical brain networks:

More specifically:

1. Exploration of speech and non-speech sound processing networks during audio-drama listening in sighted and early-blind subjects (I and II).
2. Investigation of spatial variability in functional brain networks of sighted and early-blind subjects (III).
3. Investigation of how TMS of the individually variable connection between the prefrontal cortex and primary somatosensory cortex influences tactile processing (IV).

4. Methods

4.1 Subjects (I−IV)

The subjects of studies I–IV participated after signing an informed consent. For all four studies, we received approval from the ethics committee of the Helsinki and Uusimaa Hospital District. Table 1 gives an overview of the subjects included in each study.

Table 1. *Overview of the subjects included in studies I−IV.*

Study	Number of subjects		Age range (years)		Method
	Blind	Sighted	Blind	Sighted	
I	n/a	13	n/a	19–30	fMRI during naturalistic auditory stimuli
II	7	16*	19–43	19–37	fMRI during naturalistic auditory stimuli
III	7**	7***	19–43	19–37	fMRI data collected during rest and naturalistic auditory stimuli
IV	n/a	8	n/a	23–31	DTI and tractography to find tracts combining the PFC and S1; TMS of the tracts during a tactile discrimination task

* Included 13 subjects from study I
** The same subjects as in Study II
*** Sampled from the 16 subjects in Study II

Fifteen healthy right-handed adults participated in Study I. However, since we excluded one subject because of excessive movements during audio-drama scanning and another because the subject could not recall the storyline, we included 13 subjects (six women, seven men) in the analysis.

Studies II and III included seven early-blind subjects (four women, three men; six right-handed, one ambidextrous by report; see Table 2 for the causes and durations of the blindness), and seven age- and gender-matched sighted subjects (four women, three men; all right-handed by report). We were unable to attain the Edinburgh Inventory score for one sighted subject. The means of the Edinburgh Inventory scores were similar between the groups (two-sample t-test, $p = 0.58$): the mean for the blind group was 61.4 (range −35–100), and for the sighted group the mean was 71.3 (range 45–100). All blind subjects read Braille (4.9 ± 2.6 hours/week, mean ± standard deviation; range 2–8 hours). The resting-state data of 16 sighted subjects (seven women, nine men; all right-handed by report) were used to compute the reference distribution in Study II. All subjects were native Finns and fluent in Finnish.

Table 2. *Causes and duration of the blindness of the early-blind subjects*

Age when blind	Cause of blindness
Since birth	Norrie's disease, no other neurological deficits
Since 3 years of age	Cataract, aniridia
Since birth	Leber's congenital amaurosis
Since birth	Leber optic atrophy
Since 6 months of age	Retinopathy of prematurity
Since 3 years of age	Retinopathy of prematurity
Since birth	Retinopathy of prematurity

Eight healthy right-handed volunteers participated in Study IV (three women and five men). Five of the subjects participated in all three main experiments; three subjects participated in two experiments.

4.2 Audio drama stimulus, data acquisition and preprocessing (I−III)

The stimulus used for studies I, II and III was derived from a Finnish movie called "Letters to Father Jaakob" (Postia Pappi Jaakobille, director Klaus Härö, Production company: KinotarOy, Finland, 2009). The stimulus duration was 18 min 51 s. Speech played mostly in the foreground and was on average 3.9 dB louder than the non-speech sounds, although non-speech sounds occurred more frequently, for roughly 65% of the stimulus duration compared with speech that occurred for 60%.

In the movie, a woman released from prison is employed at an old dilapidated clergy house; her task is to help an old blind priest read and write letters. The audio drama included sounds from the original movie and a narration describing the surroundings and the actors' actions. The scenes that were used for the stimulus included a dialogue between the employed woman and the priest, and between the priest and a mailman. The soundscape consisted of music and natural outdoor and indoor sounds, such as birdsong and creaking doors.

For Study I, MIRtoolbox was used to extract envelopes showing sound power over time, with a sampling rate of 3000 Hz, from the original soundtrack of the movie. The dialogue and the narration were extracted into one amplitude envelope and all other

sounds into another amplitude envelope. These amplitude envelopes were used as the speech (dialogue and narration) and non-speech (mostly music) regressors in Study I and were convolved with a hemodynamic response function, then down-sampled to the fMRI sampling rate (0.4 Hz) (Brennan et al., 2012). The resampling steps contained anti-aliasing filters.

The dialogues were recorded while the scenes were acted; thus, some non-speech sounds such as steps and the clatter of coffee cups were part of the speech regressor. Since such sounds might be more meaningful for blind than sighted subjects, and it was especially important to address speech processing in Study II, the soundtrack was manually annotated using 1-s frames. Frames containing speech were labeled as one and the other frames as zero. The resulting boxcar model was convolved with a hemodynamic response function and resampled to the fMRI sampling rate (Lahnakoski et al., 2012).

For studies I, II and III, we obtained the MRI data with identical parameters using a Signa VH/i 3.0 T MRI scanner (General Electric, Milwaukee, WI, USA). We collected the anatomical images with a T1-weighted 3D-MPRAGE sequence with repetition time (TR) = 10 ms, echo time (TE) = 30 ms, preparation time = 300 ms, flip angle = 15°, field of view = 25.6 cm, matrix = 256 × 256, slice thickness = 1 mm, voxel size = 1 × 1 × 1 mm^3, and number of axial slices = 178. Next, we collected fMRI data during ~10-min (240 volumes) resting-state and ~19-min (456 volumes) audio drama scans using gradient EPI sequences with the following parameters: TR = 2.5 s, TE = 30 ms, flip angle = 75°, field of view = 22.0 cm, matrix = 64×64, slice thickness = 3.5 mm, voxel size = 3.4 × 3.4 × 3.5 mm^3 and number of oblique axial slices = 43. We instructed the subjects to lie still with eyes closed during scanning, and to listen attentively when presented with the audio drama.

Before brain imaging, subjects listened to a 9-min introduction about the main characters and the scenery, to induce a similar mindset across subjects. Next, crude hearing thresholds were determined with a method-of-limits approach. A sound (5 sinusoidal tones of 300, 700, 1000, 1350, and 1850 Hz; duration 50 ms) was presented binaurally in descending and ascending order with 5 dB steps, and the process was repeated until we found a threshold measure where the subject reported hearing ≥ 70% of the sounds. During scanning, subjects heard the stimulus binaurally through a UNIDES ADU2a audio system (Unides Design, Helsinki, Finland) from a PC with an audio amplifier (Denon AVR-1802) and a power amplifier (Lab.gruppeniP 900). Eartips (Etymotic Research, ER3, IL, USA) were inserted into the subjects' ear canals and connected to plastic tubes that delivered the sounds. Earmuffs provided further hearing protection from the scanner background noise.

In studies I–III, the following steps were taken to preprocess the fMRI data: realignment, slice timing correction (not in Study I), coregistration of the functional images to the anatomical images, normalization to Montreal Neurological Institute (MNI) space, and smoothing with a full-width-at-half-maximum (FWHM) Gaussian kernel. In Study I and II, the images were normalized into 3.5-mm isotropic voxels using SPM8. In Study III, the data were preprocessed using the freesurfer FS-FAST pipeline, and normalized into 2-mm isotropic voxels. A 8-mm FWHM Gaussian kernel was used for smoothing the data in Study I, and a 12-mm kernel was used for smoothing the data in

Study II and III. A larger smoothing kernel was chosen for Study II and III in order to adequately estimate the individual subjects' independent components (Allen et al., 2012) and to achieve better alignment between the blind and sighted subjects.

4.3 Independent component analysis, and measuring connectivity and inter-subject variability of independent components (I, III)

For studies I and III, the Infomax algorithm (Lee et al., 1999) implemented in the group ICA toolbox GIFT v1.3 (http://icatb.sourceforge.net/) was used to estimate the spatial maps and time-courses corresponding to the independent components. A minimum-description-length algorithm estimated the mean number of sources in the audio-drama data as 51 (I), and 53 in the resting-state data (III) (Li et al., 2007). The ICASSO method was used to assess the replicability of the independent components in studies I and III (Himberg et al., 2004). The toolbox performed back-reconstruction to individual components with the GICA3 algorithm (Erhardt et al., 2011).

In Study III, independent components located in the gray matter (Stevens et al., 2007) were identified. Gray matter components were considered as those that had substantial overlap (> 67%) with a binarized gray matter SPM8 MNI-template.

In Study III, the aim was to determine whether inter-subject spatial variability of some functional networks differed between blind and sighted subjects. The assumption was that, congenitally, functional networks are rather similar (Fransson et al., 2007), but experience-dependent plasticity is more likely to increase than decrease the inter-subject spatial variability of functional networks. Thus, functional networks undergoing strong plasticity following early-onset blindness should be less correlated between blind than sighted subjects. In contrast, functional networks that are used less following early-onset blindness should have less inter-subject spatial variability in the group of blind than in the group of sighted subjects. To test this assumption, pairwise Pearson's correlations were calculated between all pairs of subjects, separately for the blind and sighted subjects, for each ICA-derived unthresholded spatial map. Next, we compared the resulting 21 pairwise correlation values between the groups with a Mann-Whitney test resulting in a U-value. The analysis was done both for the resting-state data and the first ten minutes of the data collected during the audio drama.

The p-values were estimated using a reference distribution based on real data of all 16 normally-sighted subjects. The reference distribution was estimated in the following manner: a sample of 14 subjects was taken without replacement from the 16 subjects and then randomly divided into two groups of seven subjects. The computer ran the ICA for the sample with the same parameters as in the blind versus sighted comparison and computed the inter-subject correlations for all pairwise comparisons for each spatial map in both groups. A Mann-Whitney test compared the resulting pairwise correlation values between the groups. The computer repeated the process for all 120 possible combinations of selecting 14 subjects out of 16, resulting in a total of 6,360 values in the reference distribution. The frequencies of the reference distribution values were then used to

compute FDR-corrected p-values corresponding to the U-value gathered for the spatial maps.

Although the maps derived from spatial ICA are spatially independent, their time-courses can exhibit temporal dependencies, providing information about functional network connectivity (FNC) (Jafri et al., 2008). In both Study I and III, FNC was assessed by correlating—within each subject—the time-courses of chosen independent components with the time-courses of the other independent components. After determining the Pearson's correlation coefficient, a Fisher transformation was applied, and a two-tailed one-sample t-test was used to identify significant correlations at the group level (I, III), or a two-sample t-test to identify differences in FNC between the groups of sighted and blind subjects (III).

4.4 Computing the inter-subject correlation map and sorting the independent components with the ISC map and the speech and non-speech sound regressors (I, II)

In Study I and Study II, an inter-subject correlation (ISC) map (Hasson et al., 2004) was computed to find cortical areas related to audio-drama listening (Malinen & Hari, 2011). For the ISC calculation, the effects of the six realignment parameters, linear drift, and the global mean signal were removed from the data. Then, the correlation images of all subject pairs were computed by first determining the Pearson's voxel-by-voxel correlation coefficients followed by a Fisher transformation to convert the correlation coefficients to normally-distributed values. In Study I and II, correlation images for all subject pairs were used to search for statistically significant correlations within the groups (one sample t-test), and in Study II, between the groups (two-sample t-test). Clusters exceeding the threshold $p < 0.01$ (family wise error (FWE)-corrected) and the extent of 20 voxels were considered to be statistically significant. No values in a distribution computed for the resting-state data (see section 4.2) exceeded these thresholds.

In Study I, independent components with stimulus-related characteristics were identified with the GIFT software by sorting the ICA-derived spatial maps according to their spatial correlations with the thresholded ISC map (Malinen & Hari, 2011). Spatial maps with > 0.3 correlation and > 50% overlap with the ISC map were considered task-related. Additionally, to estimate the reactivity to speech and non-speech sounds, the time-courses of the task-related independent components were entered in a multiple regression analysis comparing them with the speech and non-speech regressors.

4.5 Measuring hemisphere dominance for speech sounds using a whole-brain and regions of interest approach (II)

For Study II, the LI-toolbox was used to estimate whole-brain lateralization indices (Wilke & Lidzba, 2007; Wilke & Schmithorst, 2006). The lateralization index compares the

amount of activation in one hemisphere to the other hemisphere; the lateralization index ranges from −1 (right-sided) to 1 (left-sided). First, for each subject, correlations with the speech regressor were assessed by performing a general linear model analysis. The influence of the regressors of no interest was removed, namely, the non-speech regressor, a constant, the mean white-matter signal, the mean cerebrospinal fluid signal, the 6 rotation regressors, a full wavelength sine and cosine waveform, and a linear drift term. The individual speech sound t-maps were entered into the LI-toolbox and were used to subtract the sum of the activation values in the right hemisphere from those in the left hemisphere, and then divided by the sum of the whole-brain activation. The procedure was repeated using several bootstraps and different t-map thresholds (Wilke & Lidzba, 2007; Wilke & Schmithorst, 2006), resulting in weighted means which were compared between the groups with a two-sample t-test (two-sided).

For the region of interest (ROI) approach in Study II, the histological probability maps provided in the Anatomy toolbox (Eickhoff et al., 2005) were used to construct four ROIs depicted in Figure 3. The histological maps of the primary auditory areas labeled Te1.0, Te1.1, and Te1.2 (Morosan et al., 2001) were sampled with the marsbar toolbox to a left- and right-sided mask of the auditory cortex. Additionally, a bilateral ROI was constructed encompassing the posterior two-thirds of the superior temporal gyrus, labeled Te3 (Morosan et al., 2005). The Te3 is functionally defined by strong reactivity to narratives, especially in the left hemisphere (Schmithorst et al., 2006). Since the primary visual areas display activation during verbal memory tasks (Amedi et al., 2003), the primary visual areas were defined as another ROI (Amunts et al., 2000). Furthermore, the Anatomy toolbox provided an ROI encompassing the lateral aspects of the anterior occipital lobe, named hOC5 (Malikovic et al., 2007). This area corresponds to the motion-sensitive visual area (Wilms et al., 2005) known to react to speech (Burton et al., 2003; Burton et al., 2002b) and tones (Watkins et al., 2013) in blind subjects.

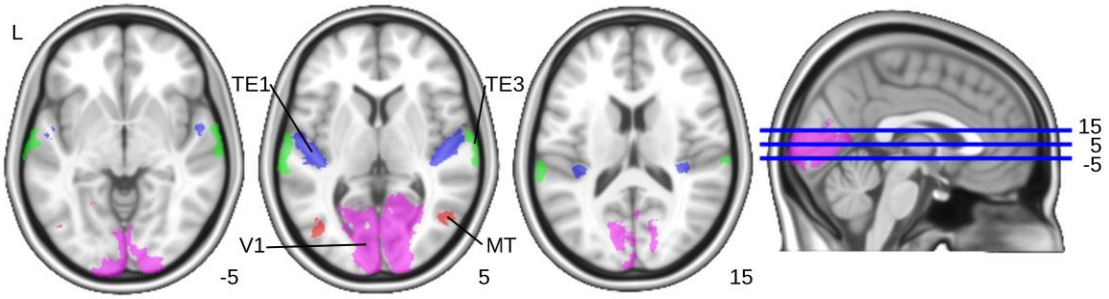

Figure 3 *The four regions of interest (ROIs) used in Study II provided by the Anatomy toolbox (Eickhoff et al., 2005). The blue ROI is composed of the TE1.1, TE1.2 and TE1.3 areas and represents the primary auditory cortex. The green ROI, composed of the TE3, encompasses the posterior two-thirds of the lateral superior temporal gyrus. The purple ROI encompasses the primary visual areas (V1). The red ROI consists of the Hoc5, encompassing the lateral anterior occipital gyrus, and is functionally equivalent to the motion-sensitive visual area (MT). The numbers indicate the MNI z-coordinates. L = left*

To estimate whether the hemispheres of blind and sighted subjects could be discriminated by their reactivity to speech or non-speech sound, the following analysis was performed: first, the time-course of each voxel in the three ROIs was averaged in both hemispheres separately. A partial correlation analysis comparing the resulting six time-courses with either the speech or non-speech regressor was performed. The effect of the nuisance regressors was removed from the data, namely, a constant, the global mean signal of the white matter and the cerebrospinal fluid, the 6 rotation regressors, a full wavelength sine and cosine waveform, a linear drift term and either the speech or non-speech regressor. Next, a two-way repeated measures ANOVA was performed to investigate the main effects of hemisphere (left or right) and group (blind or sighted). Post hoc tests (t-tests) were performed when appropriate with Bonferroni correction of the resulting p-values.

4.6 Diffusion tensor imaging, tractography, and transcranial magnetic stimulation to assess the role of the prefrontal cortex in tactile discrimination (IV)

Study IV consisted of four stages. First, subjects underwent DTI. Next, TMS was used to determine the location of the thenar skin representation area in the primary sensory cortex (S1). In the third stage, we assessed tracts from the S1 area to the prefrontal cortices with tractography. In the main experiment, subjects performed a tactile temporal discrimination task while we stimulated the DTI- and tractography-informed S1-PFC links with TMS.

The MRI data were obtained with the Signa VH/i 3.0 T MRI scanner (General Electric, Milwaukee, WI, USA) used for studies I–III. First, a structural image set was acquired using a T1-weighted 3D anatomical volume with a field of view = 240 mm, matrix = 256 × 256, voxel dimensions = 0.9 × 0.9 × 1.0 mm^3, TE = 1.9 ms, TR = 9.1 ms, IT = 300 ms, flip angle = 15° and NEX = 2, and number of axial slices = 162. We acquired the DTI data with an 8-channel high-resolution brain array head coil (GE Signa Excite, GE Healthcare, Chalfont St.Giles, UK). The DTI scheme consisted of acquiring a set of 60 diffusion-weighted images with non-collinear diffusion gradients (1000 s/mm^2, Δ = 30 ms, δ = 24 ms) and four non-diffusion-weighted images. A set of 54 slices was acquired using a matrix of 128 × 128 and voxel dimensions of 1.9 × 1.9 × 3.0 mm^3, rectangular FOV = 240 mm, TE = 79 ms, and TR = 10,000 ms. A manually-adjusted higher-order shim procedure was performed prior to the acquisition of the DTI data. The imaging was performed twice, resulting in a data set consisting of 128 volumes.

The data were processed with the FSL software (www.fmrib.ox.ac.uk/analysis/). The FMRIB's diffusion toolbox (FDT) corrected the DTI dataset for subject motion and eddy currents using the non-diffusion-weighted volume as a reference. Next, to allow probabilistic tractography, the BEDPOSTX tool was used to obtain a Bayesian estimation of the diffusion parameters (Behrens et al., 2003a; Behrens et al., 2003b). The skull-stripped non-diffusion and anatomical T1-weighted volumes were coregistered with each other.

After functional determination of the somatosensory cortex hotspot (S1hs), located at the coordinates where TMS blocked a tactile sensation from the thenar area (see below),

the connections from the S1hs to the PFC were probed in the following manner: the coordinates for the S1hs were transferred to the anatomical T1 image, registered to the diffusion space. A mask corresponding to the S1hs, with a diameter of approximately 10 mm, was used as a seed for tractography. Tracts starting from the seed mask (step length = 0.5; number of steps = 2000; number of particles = 5000; curvature threshold = 0.2) were computed; thus, each voxel attained a connectivity value corresponding to the number of streamlines passing from the seed region through the voxel. We first adjusted the threshold to a connectivity value > 100 (Ciccarelli et al., 2006), but had to reduce it in one subject to 48 to find a solid tract to the superior frontal gyrus (SFG), and in another subject to 30 to find a solid tract to the middle frontal gyrus (MFG). Here, MFGhs and SFGhs refer to the most anterior PFC sites in the MFG and SFG, respectively, with a tractography-informed connection with the S1hs.

The experiments employing TMS consisted of three parts: (i) determining the TMS motor threshold, (ii) finding the thenar representation site in S1, and (iii) the tactile temporal discrimination task. We delivered monophasic TMS pulses with the eXimia NBS system (Nexstim Ltd. Helsinki, Finland), employing an optical tracking system and displaying the location of the TMS coil on the individual MR images. TMS pulses were applied to the left hemisphere, i.e. contralateral to the tactile stimuli. TMS intensity was determined by mapping the primary motor cortex to find a location producing a motor response from the relaxed abductor pollicis brevis muscle. First, the coil position producing a motor response was determined while measuring motor evoked potentials with continuous on-line surface electromyography. After determination of the optimal coil position, the primary motor cortex was stimulated with sets of 10 TMS pulses; the stimulation strength was adjusted between sets. The resting-motor threshold was defined as the lowest TMS intensity at which $\geq$ 5 out of 10 pulses produced a motor evoked potential of $\geq$ 50 μV. We applied TMS at 120 % of the resting motor threshold during the tactile discrimination tasks. The stimulation strength was on average 65 % ± 12.4 % of the maximal output of the stimulator.

For both the S1 blocking and the tactile discrimination task, two Ag-AgCl skin electrodes (Ambu, Ballerup, Denmark) were attached to the thenar or hypothenar area of the dominant hand. A Grass PSIU6 constant-current stimulator (Grass Instruments, Quincy, MA) delivered 0.2-ms electrical stimuli at threshold intensity. The subjects' tactile threshold for single pulses was determined by the method of limits, and was defined as the intensity the subjects felt in at least 90% of the trials.

The thenar representation site in S1 was determined using a blocking experiment (Hannula et al., 2005). The Grass stimulator delivered electrical test stimuli at threshold intensity to the thenar skin of the right hand while applying single TMS pulses at 120% of the motor threshold with a 20-ms delay after delivering the cutaneous test pulse. Subjects answered 'yes' after each TMS pulse if they felt a tactile stimulus, 'no' if not, and 'maybe' if they were uncertain. We probed the S1 cortical area with TMS until the S1hs was found, i.e., the location at which TMS stimulation blocked at least 75% of the cutaneous test pulses.

In the tactile temporal discrimination task, cutaneous single or twin test stimuli were applied to the thenar or hypothenar area of the dominant hand at double the threshold

intensity. The interstimulus interval of the twin pulses was determined individually based on a preliminary study on how subjects discriminate a single pulse from a twin pulse in about 90% of stimulus presentations (Pastor et al., 2004). This interstimulus interval was most often 90 ms. During the tactile temporal discrimination task, subjects indicated with a button press of a computer mouse, and verbally, whether they felt a single pulse or a pulse pair, while a single TMS pulse was applied to the MFGhs, SFGhs or approximately 5 cm above the head (sham TMS).

Three main experiments were performed: first, the effect of temporal delay between tactile stimulation and TMS on temporal discrimination was assessed using three different delays (0 ms, 20 ms or 50 ms from the second pulse). Secondly, the role of the PFC subregions in top-down modulation of tactile processing was assessed by comparing the temporal discrimination ability during TMS of the MFGhs, SFGhs, and the sham TMS. Thirdly, the effect of TMS on tactile discrimination ability in the hypothenar area was determined during stimulation of the MFGhs-S1 link previously probed for the thenar S1hs. The delay from the delivery of the second cutaneous test pulse to the delivery of the TMS pulse was 0 ms in the two latter experiments.

Within one experimental condition, the tactile pulse was delivered to either the thenar or hypothenar skin area. TMS pulses were delivered to MFGhs, SFGhs or five centimeters above the head (sham). Every experimental condition consisted of presenting both the cutaneous single pulse and the twin pulses eight times. The experimental conditions were counter-balanced between and within subjects and lasted 2−3 min; the subjects had the possibility to rest between conditions. The tactile threshold was measured once in a while to exclude the possibility that a change in the threshold contributed to the results.

To assess the subject's capacity to discriminate between single and twin pulses, we performed a receiver operating characteristics (ROC) curve analysis (Swets, 1973) using MedCalc (Mariakerke, Belgium) software. Reporting one pulse when the stimulus was a single pulse was considered a hit, but reporting two pulses was a false alarm. Similarly, reporting two pulses for a twin pulse was considered a hit, but reporting one pulse was a false alarm. For each condition, a ROC curve was created by comparing responses to single and twin pulses. The area under the curve (AUC) was used as an index of the subject’s discriminative capacity. In the ROC analysis, the AUC value varies from 0.5 to 1.0: the value 0.5 indicates that the subject’s discrimination of a single pulse within a twin pulse is at chance level, whereas the value 1.0 indicates no false alarms. The AUC values were entered into a one- or two-way repeated measures ANOVA. Post hoc Tukey’s tests were used when appropriate.

5. Results and discussion

5.1 Study I

Study I used naturalistic stimuli derived from an audio drama to search for speech and non-speech sound processing areas in the brain. The ISC map, shown in Figure 4, revealed the areas where the subjects' brains showed similar temporal fluctuation during the audio drama. The ISC map was employed to find task-related independent components. The ISC map consisted mainly of four independent components: IC1, centered on Brodmann area 22 and included Heschl's gyrus, the superior temporal gyrus (STG), the Rolandic operculum, and the posterior insula (correlation with ISC map = 0.67, overlap with ISC map = 97%). IC2, located medially from IC1, encompassed bilaterally the primary auditory cortices including the STG (correlation with ISC map = 0.52, overlap with ISC map = 87%). IC3 encompassed the middle temporal gyrus, STG, angular gyrus, inferior temporal pole and orbital part of the inferior frontal gyrus (IFG) in the left hemisphere (correlation with ISC map = 0.40, overlap with ISC map 70%). IC4 encompassed the right MTG, STG and inferior temporal pole (correlation with ISC map = 0.40, overlap with ISC map 90%). Comparing these four independent components with the speech and non-speech sound regressors revealed that IC1 and IC2 reacted to both speech (partial r = 0.47 and 0.22) and non-speech (r = 0.10 and 0.12) sounds, and were named the all sounds components. The two other components (IC3 and IC4) reacted only to speech sounds (r = 0.28 and 0.23), and were, therefore, called the speech components.

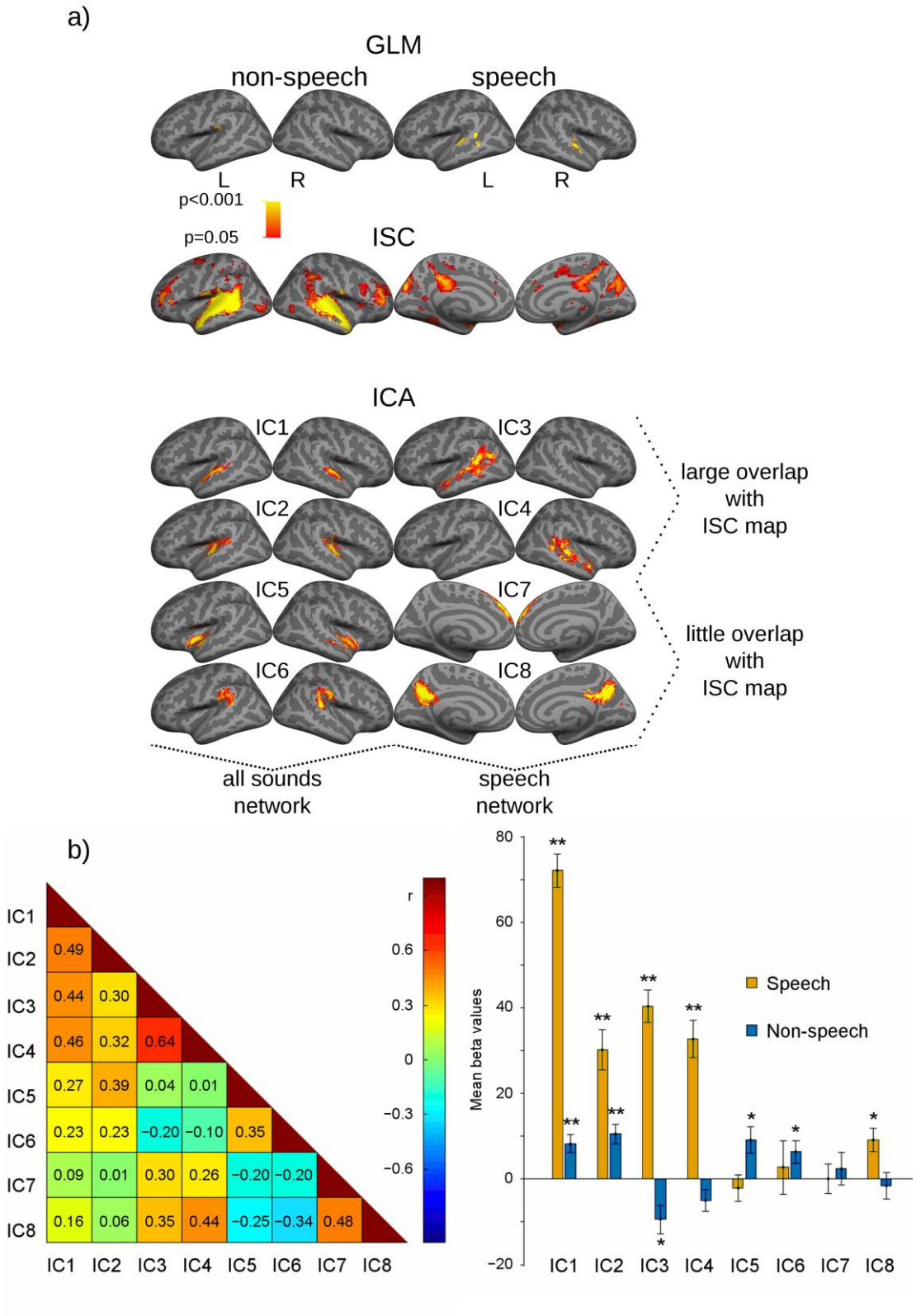
a)
GLM
non-speech
speech
L
R
L
R
p<0.001
p=0.05
ISC
ICA
IC1
IC3
IC2
IC4
IC5
IC7
IC6
IC8
large overlap with ISC map
little overlap with ISC map
all sounds network
speech network
b)
IC1
IC2 0.49
IC3 0.44 0.30
IC4 0.46 0.32 0.64
IC5 0.27 0.39 0.04 0.01
IC6 0.23 0.23 −0.20 −0.10 0.35
IC7 0.09 0.01 0.30 0.26 −0.20 −0.20
IC8 0.16 0.06 0.35 0.44 −0.25 −0.34 0.48
IC1 IC2 IC3 IC4 IC5 IC6 IC7 IC8
r
0.6
0.3
0
−0.3
−0.6
Mean beta values
80
60
40
20
0
−20
Speech
Non-speech
IC1 IC2 IC3 IC4 IC5 IC6 IC7 IC8

Figure 4 *Results from Study I. a) The first row shows the GLM-derived maps, the second row the ISC map and the third to sixth rows show the ICA-derived spatial maps. Independent components IC1–IC4 overlapped with the ISC map, while IC5–IC8 showed little overlap with the ISC map. Here, IC1, IC2, IC5 and IC6 appear to compose a network reacting to all sounds while IC3, IC4, IC7 and IC8 compose a network reacting only to speech. b) Despite little reactivity to either speech or non-speech sounds, IC5 and IC6 correlated with IC1 and IC2, while IC7 and IC8 correlated with IC3 and IC4. Thus, IC5–IC8, which did not overlap with the ISC map, seemed stimulus-related, but the relationship to the stimulus was unique in each subject. This picture is modified from (Boldt et al., 2013). The CCAL license applies to the material. N = 13.*

The independent components overlapping with the ISC map showed rich connectivity with the independent components not overlapping with the ISC map. The FNC analysis revealed connectivity between the all sounds components (IC1 and IC2) and two components not overlapping with the ISC map: i) IC5 (correlation with ISC map = 0.10), which encompassed the supramarginal gyrus; and ii) IC6 (correlation with ISC map = 0.13), encompassing the STG bilaterally and extending to the Rolandic operculum, superior TP, putamen and insula. Both of these components encompassed areas involved in shifting attention based on auditory cues (Baumann & Greenlee, 2007; Cauda et al., 2011). The FNC analysis also indicated connectivity between the speech components (IC3 and IC4) and two other independent components not overlapping with the ISC map: i) the precuneus/cuneus (IC7, correlation with ISC map = 0.01) and ii) the middle and superior frontal gyrus (IC8, correlation with ISC map = 0.02). These two components encompassed areas participating in semantic processing (Wilson et al., 2008), and might integrate speech on a time-scale > 30 seconds (Lerner et al., 2011).

The independent components overlapping with the ISC map showed a strong relationship to the stimuli, while the four components (described in the previous paragraph) which did not overlap with the ISC map were weakly or not at all stimulus-related. The anatomical distribution of the components that overlapped with the ISC map and the stimulus-related components that did not overlap with the ISC map coincided with the proposed division of the brain into two large-scale networks. One of these networks is considered to react to external stimuli, the other is considered to process internal thoughts (Golland 2007; Golland 2008). Interestingly, the present results suggest that networks reacting to external stimuli are perhaps functionally connected with the networks processing internal thoughts, but in a unique manner for each subject.

The results suggested that two distinct large-scale networks process naturalistic sounds, one network processing speech, the other processing both speech and non-speech sounds. The stimulus-related networks seemed to encompass areas that reacted to stimuli in a similar manner in each subject, but also areas with high temporal variability between subjects.

5.2 Study II

Previous findings suggest that the right hemisphere reacts more intensely to speech sounds in blind than in sighted subjects (Röder et al., 2000; Röder et al., 2002). Study II asked whether the difference in hemispheric reactivity is coupled with a different amount of lateralization to speech and non-speech sounds in blind and sighted subjects. We used a naturalistic audio drama to explore the lateralization of both speech and non-speech sounds in a group of blind and sighted subjects. The whole-brain analysis revealed left-lateralized responses to naturalistic speech sounds in sighted subjects (mean LI = 0.49). The responses were on average slightly right-lateralized in the blind subjects (mean LI = –0.11); the mean LI was significantly different between the groups ($p = 0.0016$).

The ISC map, shown in Figure 5, revealed the areas where the subjects' brains showed similar temporal fluctuation during the audio drama. The ISC map encompassed fewer areas than the ISC map in Study I, presumably because of fewer subjects in Study II. In blind compared with sighted subjects, the ISC was significantly stronger in the junction of the superior and middle temporal gyrus in the right hemisphere. In the sighted compared with blind subjects, the ISC was significantly stronger in the left primary auditory areas.

In sighted subjects, the ROI analysis showed stronger left than right hemisphere responses to speech sounds both in the primary auditory cortices ($r_{left} = 0.56$, $r_{right} = 0.48$) and the lateral temporal gyrus ($r_{left} = 0.65$, $r_{right} = 0.55$). In blind subjects, the hemispheric reactivity was similar on the right and on the left both in the primary auditory cortex ($r_{left} = 0.37$, $r_{right} = 0.45$) and the lateral temporal gyrus ($r_{left} = 0.52$, $r_{right} = 0.52$). A significant group × hemisphere interaction effect suggested different left and right hemisphere responses to naturalistic speech sounds in blind compared with sighted subjects. The interaction effect was significant both in the primary auditory cortex ($F(1,12) = 13.21$, $p = 0.0034$) and in the lateral temporal gyrus ($F(1,12) = 7.9$, $p = 0.016$). A main effect of group emerged in the primary auditory cortex ($F(1,12) = 5.75$, $p = 0.034$), and of hemisphere in the lateral temporal gyrus ($F(1,12) = 8.22$, $p = 0.014$). The responses to speech were overall stronger in the left primary auditory cortex of sighted than blind subjects. Furthermore, the lateral surface of the anterior occipital lobe reacted to speech more vigorously in the blind ($r_{left} = 0.20$, $r_{right} = 0.21$) than in the sighted subjects ($r_{left} = -0.08$, $r_{right} = -0.03$; $F(1, 12) = 56.18$, $p < 0.0001$).

In sighted subjects, the ROI analysis showed similar left and right hemisphere responses to non-speech sounds, both in the primary auditory cortex ($r_{left} = 0.09$, $r_{right} = 0.13$) and the lateral temporal gyrus ($r_{left} = -0.0028$, $r_{right} = 0.08$). In blind subjects, the hemispheric reactivity was similar on the right and left in the primary auditory cortex ($r_{left} = 0.18$, $r_{right} = 0.14$), and in the lateral temporal gyrus ($r_{left} = 0.21$, $r_{right} = 0.20$). A significant effect of group emerged in the lateral temporal gyrus ($F(1,12) = 5.63$, $p = 0.035$). A significant group × hemisphere interaction effect emerged in the primary auditory cortex ($F(1,12) = 8.66$, $p = 0.012$). The lateral surface of the anterior occipital lobe was unresponsive to non-speech sounds in both the blind ($r_{left} = -0.045$, $r_{right} = -0.021$) and sighted ($r_{left} = -0.0081$, $r_{right} = -0.048$) subjects, with no significant effects revealed by the ANOVA. In blind and in sighted subjects the primary visual cortex reacted neither to speech or non-speech sounds.

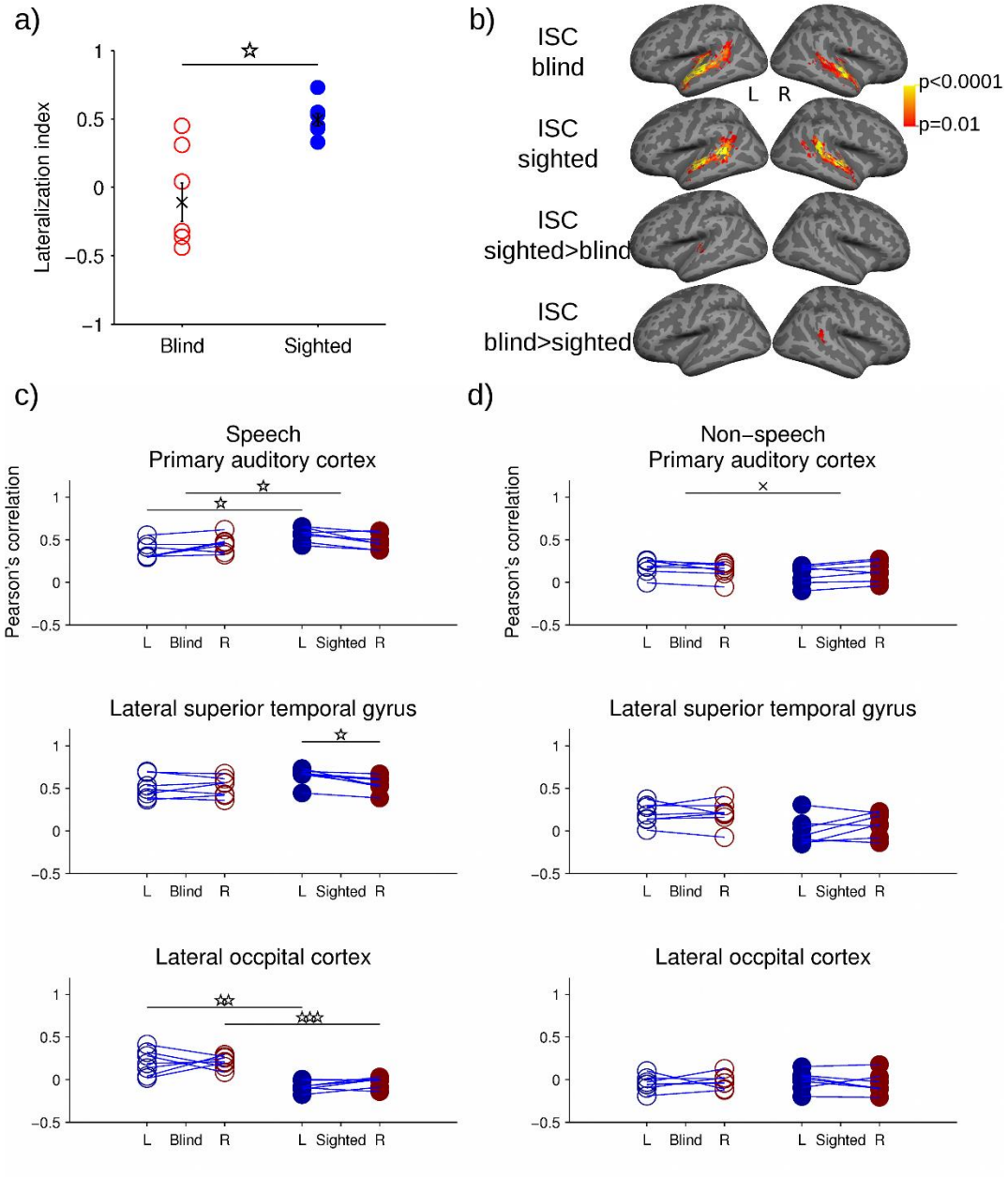

Figure 5 *a) The whole-brain lateralization index revealed that speech responses were more left-lateralized in the sighted subjects than in the blind subjects. * = 0.0016. b) The ISC analysis revealed that the left auditory cortex fluctuated more similarly in sighted than in blind subjects (peak voxel MNI-coordinates –46, –21, 10). A cluster between the junction of the right middle and superior temporal gyrus (MNI-coordinates 55, –38, 10) reacted more similarly in blind than in sighted subjects. No areas survived FWE-correction in the GLM analysis. c) and d): A two-way ANOVA showed a significant group × hemisphere interaction in the primary auditory cortex and lateral superior temporal gyrus for speech (c) and in the primary auditory cortex for non-speech sounds (d). In blind subjects the lateral occipital cortex responded to speech in both the left and right hemisphere, but remained unresponsive to non-speech sounds. Furthermore, the sighted subjects reacted stronger to speech in the left primary auditory cortex. Both groups consisted of seven subjects. P-values were corrected for multiple comparisons.× = 0.062, *p<0.05, **p<0.01, ***p<0.001.*

The reasons for the left-lateralized speech responses in most right-handed, sighted subjects remain unknown. The hemodynamic fluctuations in the right auditory cortex respond primarily to 3−6 Hz cortical oscillations, whereas the left auditory cortex responds mainly to 28−40 Hz oscillations (Giraud et al., 2007). Thus, the difference in hemispheric reactivity could emerge from the left hemisphere being better equipped to extract rapid temporal information from speech signals. Perhaps the strong responses in the right hemisphere of blind subjects result from a preserved ability to extract rapid temporal information with both hemispheres.

In conclusion, Study II showed that naturalistic speech elicits differently lateralized responses in sighted subjects compared to early-blind subjects. Both the whole-brain analysis and the ROI analysis revealed similar patterns of lateralization. Furthermore, different hemispheric reactivity to non-speech sounds in the blind compared with sighted subjects were found. These results suggest that blindness affects the development of lateralized responses to speech and non-speech sounds.

5.3 Study III

The human brain structure and function is influenced by both genetic and environmental factors (Brun et al., 2009; Glahn et al., 2010). The environmental factors seem to increase the variability of functional networks (Mueller et al., 2013). As blind people experience a world without vision, we wanted to know what parts of the brain have changed the most in blind compared with sighted subjects. Study III compared differences in inter-subject spatial variability of ICA-derived spatial maps between early-blind and sighted subjects, the search was limited to the 25 resting-state and 24 audio-drama gray-matter independent components. Here I focus on the most correlated pairs of independent components that displayed significant spatial variability differences between the groups during both the resting-state and audio-drama scan. Three gray-matter components exhibited different amount of variability between the sighted group and the blind group in the resting-state and audio-drama data; these components are shown in Figure 6. Two of the components were less variable in the sighted than in the blind subjects. These were (i) an auditory component located in the superior temporal and Heschl's gyri, supramarginal and post-central gyri, the Rolandic operculum and insula (during rest, $r_{sighted} = 0.72$, $r_{blind} = 0.64$, $p = 0.0016$; during audio drama, $r_{sighted} = 0.76$, $r_{blind} = 0.65$, $p = 0.0016$, correlation between the resting-state and audio-drama components = 0.65), and (ii) a language component found in the inferior parietal gyrus, left precuneus, and the angular gyrus bilaterally (during rest, $r_{sighted} = 0.68$, $r_{blind} = 0.58$, $p = 0.0006$; during audio drama, $r_{sighted} = 0.61$, $r_{blind} = 0.53$, $p < 0.0006$, correlation between the resting-state and audio-drama components = 0.43). Additionally, one component located in the superior, medial and inferior occipital gyri was more variable in the sighted than the blind subjects (during rest, $r_{sighted} = 0.55$, $r_{blind} = 0.71$, $p = 0.0022$; during audio drama, rsighted = 0.56, $r_{blind} = 0.72$, $p = 0.0009$, correlation between the resting-state and audio-drama components = 0.62). A previous experiment comparing the spatial distribution of functional rest and task networks showed

similar correlations between resting-state and task-related networks (Smith et al., 2009) as found here between the resting-state and audio-drama components.

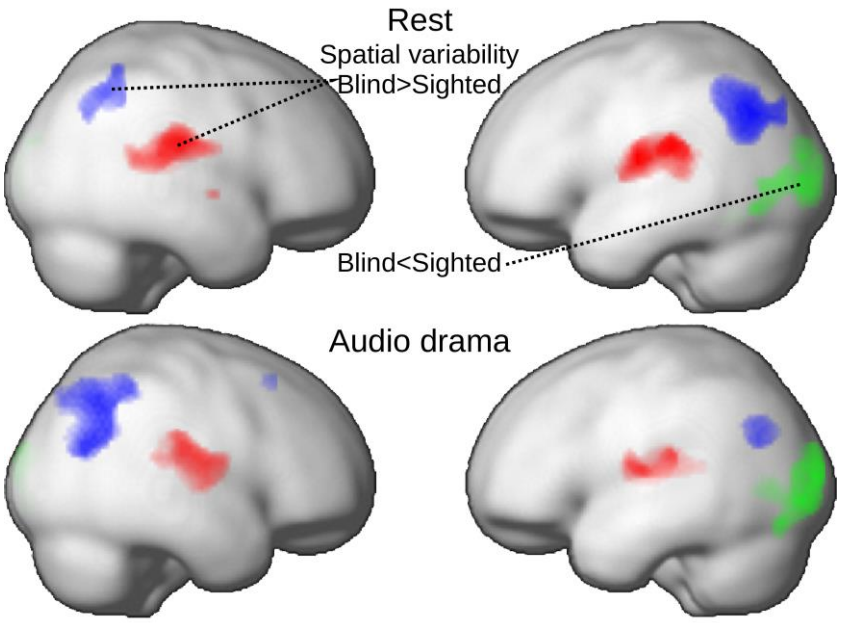

Figure 6 *Results from Study III showing the ICA-derived spatial maps that displayed inter-subject spatial variability differences between the sighted and blind subjects. The spatial maps are separately shown for the resting-state (rest) and audio-drama data. The auditory component (red) and the parietal component (blue) showed larger inter-subject variability in the blind compared with the sighted subjects. The left-lateralized lateral occipital component (green) showed less spatial variability in the blind compared with the sighted subjects. Seven subjects are included in each group. Threshold, FWE-corrected, $p < 0.01$, cluster size > 100 voxels.*

Early-blind subjects are more dependent on hearing than sighted subjects; thus, it is surprising that blind subjects perform poorly in some auditory localization tasks. These tasks thus, benefit from calibration of an intact visual system (Gori et al., 2014; Zwiers et al., 2001). However, blind people have sharper auditory spatial tuning (Röder et al., 1999) and can locate some sounds better than sighted subjects (Lessard et al., 1998), supporting the notion that compensatory changes occur in the auditory system of the blind (Bavelier & Neville, 2002). Thus, it seems plausible that the large variability in the auditory component of blind subjects reflects individual experience-dependent compensatory changes.

The angular gyrus is involved in heard (Schmithorst et al., 2006) and read (Segal & Petrides, 2013) language processing (Seghier, 2013), and, in the blind, in Braille reading (Burton et al., 2002a; Sadato et al., 1998). Perhaps the large inter-subject variability in the blind subjects could be related to reading Braille, or to the possible differences in language processing known to exist between blind and sighted subjects (Gougoux et al., 2009; Röder et al., 2000; Röder et al., 2002; Watkins et al., 2012; Watkins et al., 2003).

Since the dorsal and ventral streams (Goodale & Milner, 1992; Milner & Goodale, 2008) exist in congenitally blind subjects, it is proposed that the development of visual streams is experience-independent (Striem-Amit et al., 2012). On the other hand, it is the synaptic pruning through Hebbian reinforcement that drives visual learning (Elston et al., 2009). The relatively small spatial variability that we found in the occipital component of the blind subjects is probably due to the lack of visual information flow in the visual pathways, resulting in reduced experience-dependent synaptic pruning (Jiang et al., 2009). The occipital component also differed in the FNC between the groups. This component showed enhanced connectivity with frontal language areas ($r_{blind} = 0.35$, $r_{sighted} = -0.17$, $p = 0.004$) and another occipital component ($r_{blind} = 0.38$, $r_{sighted} = 0.01$, $p = 0.033$). Therefore, a plausible explanation for increase in functional network variability between the blind and sighted subjects is intra-modal plasticity, rather than cross-modal recruitment. We propose that, in blind subjects, functional networks related to hearing (including language processing) and touch undergo the most experience-dependent changes, whereas occipital networks that are normally related to vision—although recruited by other senses in the blind—undergo little intra-modal experience-dependent changes.

In conclusion, the inter-subject variability of functional networks differs between the groups of early-blind and sighted subjects. The differences might be due to developmental experience-dependent plasticity in the networks of these two groups.

5.4 Study IV

One explanation for why it is hard to segregate the PFC into functional areas might be the large inter-subject variability in this area. The aim of Study IV was to explore the functional subdivision of the PFC by exploring whether stimulating individually-chosen DTI- informed targets in the PFC with TMS could affect tactile processing.

A single TMS pulse applied to the MFG-S1 link impaired the subjects' ability to discriminate a double pulse from a single pulse ($F(1, 6) = 9.94$, $p = 0.02$). Similarly, the confidence ratings were reduced ($F(1, 6) = 13.15$, $p = 0.001$), though the response times were not significantly different ($F(1, 6) = 4.42$, $p = 0.080$). Additionally, the suppression of the tactile discrimination ability varied with the TMS stimulation site (whether MFG, SFG or sham; $F(2, 10) = 6.52$, $p = 0.015$). TMS stimulation of the MFG-S1 link impaired the discrimination ability more than stimulation of the SGF-S1 link (Post-hoc Tukey's test, $p < 0.05$). The subjects' performance revealed that a 0-ms delay between the cutaneous test pulse and the TMS stimulation pulse impaired tactile discrimination the most; the subjects' performance was less impaired when the delay was prolonged to 20 or 50 ms; ($F(2, 12) = 5.89$, $p = 0.017$). Since the most effective stimulation delay was shorter than the time taken for a tactile stimulus to reach S1, the TMS effect was most likely mediated through top-down modulation of the S1 cortex (Hannula et al., 2005). Moreover, tactile processing in the hypothenar area was not impaired when stimulating the MFG-S1thenar hotspot link ($F(1,7) = 9.14$, $p = 0.019$). Figure 7 shows the hotspots overlaid on

MR images (a) and bar plots (b) of the area under the ROC curves for different stimulation delays, cutaneous test sites and TMS sites (one subject).

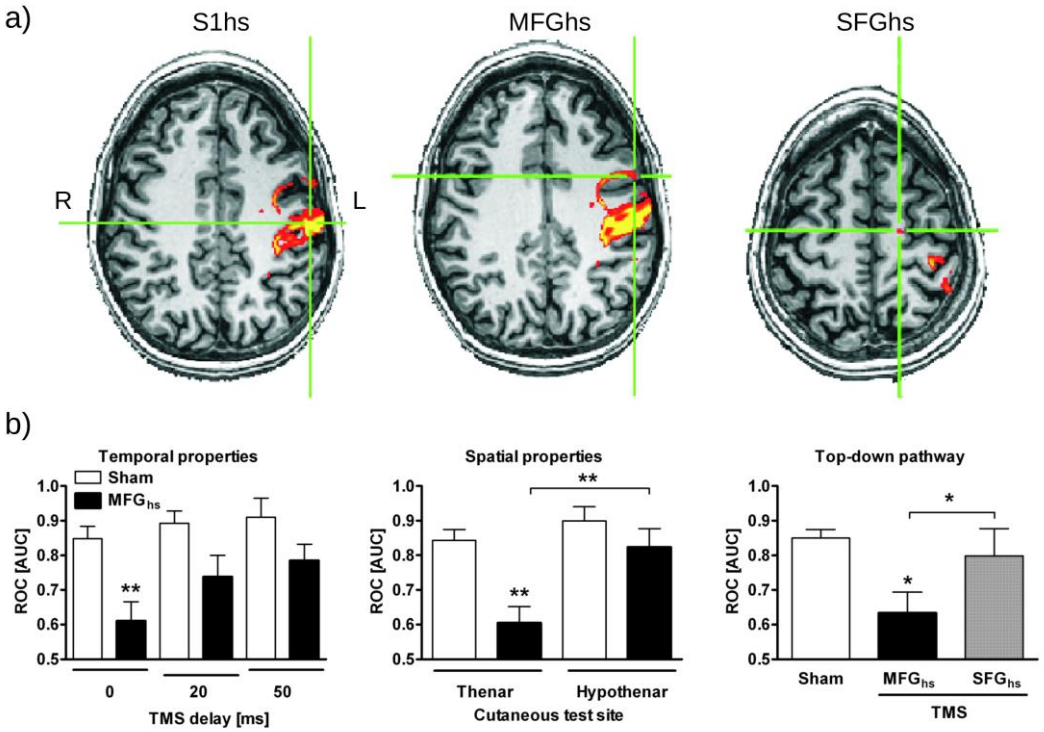

Figure 7 *a) MRI scans of one subject showing the middle frontal gyrus (MFGhs) and the superior frontal gyrus (SFGhs) hotspots with a tractography-informed link to the primary somatosensory cortex representation of the thenar skin area (S1hs). The S1hs was determined by blocking a tactile sensation with TMS and was used as a seed for diffusion tensor imaging tractography. b) First panel: TMS applied to the MFGhs impaired tactile discrimination ability more with decreasing delay between the cutaneous test pulse and the TMS stimulation. Second panel: TMS of the MFGhs impaired tactile discrimination more in the thenar area of the hand than in the hypothenar area (0-ms delay between the cutaneous stimulation and TMS). Third panel: tactile discrimination in the thenar area of the hand was impaired more by TMS of the MFGhs than of the SFGhs (0-ms delay between the cutaneous stimulation and TMS). ROC [AUC] = the area under the receiver operating characteristics curve (1 indicates perfect discrimination, 0.5 chance level discrimination). Bars show mean + standard error of the mean. * p< 0.05, ** p < 0.01 (Tukey's test; the reference is the corresponding sham group, unless specified).This picture is modified from Gogulski et al., 2013 with permission from Oxford University Press.*

TMS of the MFG-S1 link impaired discrimination of a single pulse from paired tactile pulses, whereas stimulation of the SFG-S1 link had no effect. These results support previous findings suggesting that one of the functions of the PFC is sensory gating (Hannula et al., 2010; Savolainen et al., 2011). Thus, the TMS effect could be explained in the following manner: the TMS pulse activates the MFG and the signal propagates to the S1 cortex before or simultaneously with the tactile signal from the thenar area. The MFG

activation suppresses the “distracting” temporal signal from the thenar area. The distraction results in an impaired discrimination between paired pulses and single pulses.

Figure 8 reveals that the location of the individually determined MFGhs showed considerable variation between subjects. Thus, TMS to the PFC site of the individually determined tractography-informed S1-MFGhs connection impaired performance in a tactile discrimination task even though the locations of the targeted areas showed large variability. The S1-SFG link is not involved in the described effect; thus, our findings suggest functional specialization of PFC subareas in the regulation of tactile information.

In conclusion, TMS of the MFG-S1 link impaired the subjects’ ability to discriminate between single and paired pulses. Additionally, TMS stimulation of the individually chosen tracts suppressed the discrimination of single pulses from paired pulses despite the relatively large inter-subject variability of targeted areas. The effectiveness of the TMS stimulation highlighted the advantage of using DTI-informed tracts as TMS stimulation targets.

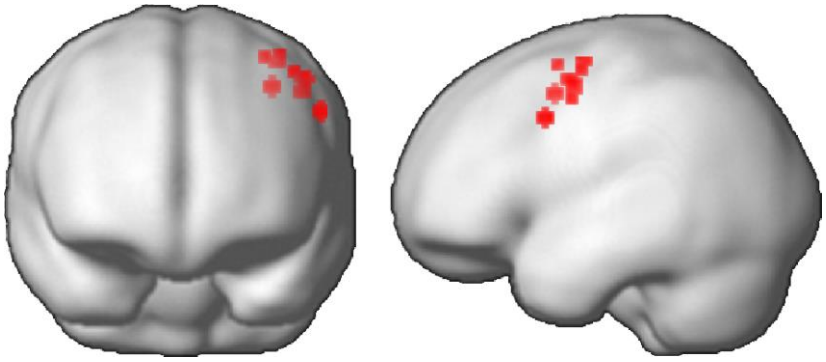

Figure 8 *The individually-normalized MFGhs locations from Study IV overlaid on an MNI template. TMS to the PFC site of the individually determined tractography-informed S1-MFGhs connection impaired performance in a tactile discrimination task even though the location showed considerable variation between subjects. The normalized coordinates of the MFGhs stimulation site can be found in supplementary tables (Gogulski et al., 2013).*

5.5 The effect of functional primary auditory cortex border variability on speech reactivity (unpublished data)

Study II showed that the auditory cortex of blind people reacted less intensively to speech than the auditory cortex of sighted subjects. Study III implicated larger inter-subject variability in the primary auditory cortex of blind than of sighted subjects. Therefore, it is plausible that, in blind subjects, the auditory cortex ROI captured the actual extent of the primary auditory cortex poorly. Thus, in blind people, the larger inter-subject variability of the auditory cortex extent could diminish reactivity to auditory sounds.

Here, I present unpublished data investigating whether increased inter-subject variability of the primary auditory cortex diminishes reactivity towards speech sounds. I

used the methods introduced for studies I, II and III. The ICA analysis was well-suited for the data-driven exploration of variability in functional networks (III). However, in this section, I focus on the histologically-delineated primary auditory cortex (Morosan et al., 2001). Therefore, I conducted a five-step voxel-by-voxel analysis of the inter-subject variability in the blind and sighted subjects' resting-state data (Mueller et al., 2013). 1) First, the effect of linear drift, white matter and cerebrospinal fluid, along with head movement, was removed from the data. 2) The time-course of each voxel within the primary auditory cortex was correlated with all other gray-matter voxels within subjects. The computation resulted in a whole-brain connectivity map for each primary auditory cortex voxel. 3) I then computed an estimate of the inter-subject variability for each primary auditory cortex voxel's connectivity maps by correlating the connectivity maps, pairwise for each voxel, between the subjects in each group. Thus, the resting-state variability could be extracted for the voxels making up the primary auditory cortex ROI. 4) Next, I computed an estimate for each subjects' variability by taking the mean of the pairwise comparison for each subject. 5) I then computed the correlations between the speech sound and primary auditory cortex time-course during audio-drama listening and assessed the relationship between the correlation with speech sounds and the mean variability for each subject's primary auditory cortex. The analysis indicated that the greater the spatial variability of the primary auditory cortex, the weaker the correlation of the primary auditory cortex with speech sounds ($r = 0.56$; $p = 0.036$, Figure 9).

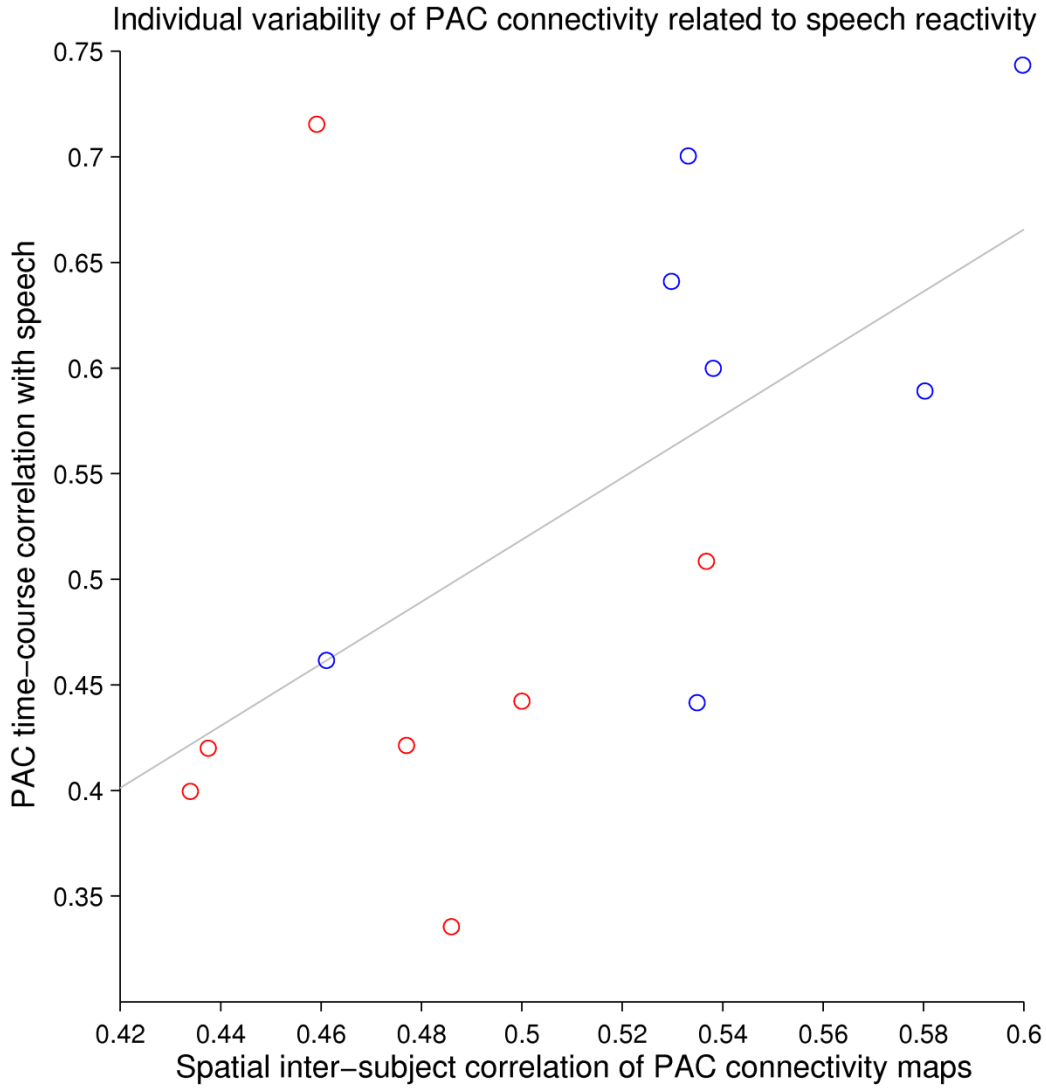

Figure 9 *The relationship between spatial variability and speech reactivity of the primary auditory cortex (PAC). The blue circles represent sighted subjects; red circles represent blind subjects. The x-axis represents the mean of the pairwise connectivity map correlations of each voxel for each subject. Less correlation represents more variability. The mean PAC correlation of each subject is correlated, within subjects, with the PAC reactivity to speech. The measures show a linear relationship ($r = 0.56$, $p = 0.036$, $N = 14$).*

I estimated the spatial variability from the resting-state data so that the measurements of reactivity to speech sounds and inter-subject variability were independent (Kriegeskorte et al., 2009). The result shown above needs further confirmation. However, weak activation of the auditory cortex in the blind subjects (as reported in Study II) could be explained by large functional variability of this area in the blind (as reported in Study III).

6. General discussion

Below, I summarize how the studies included in this thesis contributed to scientific knowledge. In addition, I discuss whether inter-subject spatial variability affects group-level responses. Furthermore, I suggest that, in the blind, the high inter-subject spatial variability of the primary auditory cortex explains the low correlations between the primary auditory cortex and speech sounds. I discuss attempts to overcome the problems caused by spatial inter-subject variability in general, and suggest that the methods used in Study IV for functional explorations of the PFC are beneficial in areas with high spatial inter-subject variability.

Study I showed that many areas of the brain responded in a similar manner in each subject to an audio drama. Stimulus-related brain responses were divided into two main networks: one reacting to both speech and non-speech sounds, the other reacting only to speech sounds. Additionally, the FNC analysis seemed to imply that some areas that are thought of as stimulus-independent (Golland et al., 2008) were responsive to the stimulus, although in a unique way in each subject. Thus, when exploring how the brain is functionally integrated to process a stimulus, functional connectivity and other related techniques contribute substantially to our understanding (Smith, 2012).

In Study II, it was shown that the left hemisphere dominance to naturalistic speech sounds is different in blind compared to sighted subjects. As expected, the left hemisphere of sighted subjects reacted more to speech than the right hemisphere. In contrast, the left hemisphere dominance to speech was not pronounced in the blind subjects. Likewise, for non-speech sounds, the hemispheres reacted differently in sighted compared to blind subjects. The left superior temporal cortex seems to support audio-visual speech integration (Calvert et al., 2001; Nath & Beauchamp, 2012; Sams et al., 1991; Szycik et al., 2012); thus, multi-sensory interaction could facilitate speech lateralization to the left hemisphere through reinforcement learning. Lack of audio-visual integration could perhaps impair the development of left-lateralized speech responses in blind subjects and explain why responses to speech sounds are bilateral, or right-lateralized, in the blind. Alternatively, supposing that left-lateralized responses are hard-wired during fetal development, multisensory integration during Braille reading could reinforce right hemisphere responses to speech in blind subjects (Nava et al., 2013; Röder et al., 2002). A voice recognition task reported stronger activation in the left hemisphere of blind compared with sighted subjects (Gougoux et al., 2009). In contrast to speech perception, voice recognition typically activates the right hemisphere more vigorously (Formisano et al., 2008). Thus, the hemispheric responses to voice recognition are perhaps also reversed in blind subjects.

Study III suggested that the spatial variability of an auditory and a parietal network is smaller in sighted than in early-blind subjects. In contrast, an occipital network showed larger spatial variability in sighted than in early-blind subjects. These findings supported the hypothesis that experience-dependent plasticity increases inter-subject variability of networks, compensating for the loss of sight. Morphological changes are apparent in the cortex of early-blind subjects. The visual cortex is thick, while the somatosensory and auditory cortex is thin (Jiang et al., 2009; Park et al., 2009). Cortical thickness is,

however, not correlated with functional network variability (Mueller et al., 2013). On the other hand, some unknown difference in the anatomy of sighted and blind subjects could cause between-group differences in functional variability. We measured the spatial inter-subject variability of functional networks with ICA since this technique can reveal similar networks during rest and tasks (Joel et al., 2011; Smith et al., 2009). With ICA, we could infer which networks had differences in group variability in both the resting-state and audio-drama data. The GICA3 back-reconstruction method used here was recommended by the group providing the GIFT toolbox used for ICA (Erhardt et al., 2011). For the variability analysis performed in Study III, the statistical independence of the back-reconstructed individual networks was important. Although GICA3 produces spatial networks with similar between-subject independence as dual regression, recent methods provide better between-subject independence (Du & Fan, 2013). In Study III, sampling the p-values from a real-data reference distribution should solve problems related to non-independence, however. Repeating the finding in two data sets was reassuring, since the sample size used in Study III was small (N = 7 in each group).

Study IV explored individual neural connections from the thenar skin representation area in the somatosensory cortex to the PFC with DTI and tractography. There is poor understanding of how the PFC gates sensory information or what the functional role of the gating is. One reason experimental information about the functional organization of the PFC is scarce might be the large inter-subject variability of the PFC (Mueller et al., 2013). Therefore, TMS combined with tractography might be an effective way to explore the functional organization of the PFC. Stimulating the prefrontal end of the MFG-S1 link with TMS while subjects discriminated single pulses from pulse pairs delivered to the thenar skin area impaired tactile discrimination. Single TMS pulses delivered to the SFG-S1 link did not impair tactile temporal processing. Together, these findings suggested that the PFC consists of functionally-specialized subareas regulating information processing.

In Study II, the auditory cortex ROI reacted less strongly to speech in the left hemisphere of blind vs. sighted subjects. High spatial inter-subject variability of the BOLD responses reduces the likelihood of obtaining a significant mean response at the group level (Speelman & McGann, 2013). Thus, as Study III suggested, higher functional variability of auditory cortex areas in blind vs. sighted subjects could explain why primary auditory areas react less strongly in blind vs. sighted subjects (Gougoux et al., 2009). The unpublished data presented in section 5.5 suggested that the weaker activation of the auditory cortex in the blind compared with the sighted subjects is proportional to larger functional variability of this area.

If individual variability weakens group-level findings, large sample sizes are required to get meaningful activation in areas with large inter-subject variability such as the PFC (Mueller et al., 2013; Speelman & McGann, 2013). Modern brain research methods provide some possible ways to overcome the problems that spatial variability exerts on the reliability of group results. Using macroanatomical landmarks to coregister the subject's anatomical images to a standard anatomical template during the normalization step helps to overcome problems related to brain shape variability. This approach improves network estimation in primary sensory areas, but not in prefrontal areas (Frost et al., 2014; Frost & Goebel, 2012). Additionally, realignment based on anatomy is insensitive to the

histological network variability (Zilles et al., 1997), and thus probably also insensitive to functional network variability. Thus, the use of ROIs based on individual histology (determined post-mortem and reported in standard space) and then sampled to MNI space would be beneficial for certain types of analysis (Eickhoff et al., 2005; Sugiura et al., 2007; Toga et al., 2006; Zilles & Amunts, 2013; Zilles et al., 2011). However, this approach requires that we have templates with probability estimates for the histological distribution of the area of interest. Even if the histological probability mapping is extended to the whole brain, different patient groups and non-neurotypical subjects could have dramatically different networks than neurotypical subjects.

ICA and related techniques could perhaps identify networks despite large inter-subject differences, and thus help in investigating areas with high spatial inter-subject variability such as prefrontal areas. Therefore, approaches using functional connectivity to aid in the normalization and alignment procedure are promising tools (Conroy et al., 2013). However, even if the underlying networks are perfectly aligned, fMRI experiments face some limitations: (i) task-related fMRI experiments only reveal the brain areas that change their level of activity during a task, not how the underlying neurons function during that task, and (ii) fMRI shows the brain areas that have a relationship with the given task; however, the causal relationship to the task remains unknown.

In contrast to fMRI, TMS can transiently disrupt activation of an area and thus interfere with the task at hand (Cowey, 2005). Thus, TMS can be used to infer whether a specific area is causally involved with the performance of a task (Bona et al., 2014). Combining TMS with MRI measurements such as fMRI and DTI has many benefits. Diffusion weighted images and tractography can enable stimulation of specific nerve bundles at an individual level, and thus improve spatial specificity and efficacy (Nummenmaa et al., 2014). Furthermore, TMS combined with tractography allows assessing causal roles of brain areas in cognitive functions. Since individual anatomy can be accounted for with structural MR images when using TMS (Bijsterbosch et al., 2012), and fMRI can be used to localize functionally active areas (Bona et al., 2014), MRI is beneficial for TMS experiments. In addition, TMS combined with individual perturbation of anatomical connectivity reveals individual anatomy even in areas with high inter-subject spatial variability such as the PFC (Hannula et al., 2010; Savolainen et al., 2011).

In summary, TMS combined with DTI and tractography has the following advantages: TMS efficiently interferes with the performance of a tactile discrimination task even when targeted areas have large inter-subject spatial variability, such as the PFC. TMS permits investigations of the causal relationship between the stimulated area and cognitive processing. Finally, TMS has excellent temporal resolution. Therefore, navigated TMS combined with imaging techniques such as DTI is a promising tool for future investigations.

7. Conclusion

In this thesis, I presented the following original contributions to neuroscience. Study I demonstrated involvement of two main networks while subjects listened to naturalistic stimuli; one reacted to both speech and non-speech sounds and the other reacted only to speech. Study II revealed different hemispheric reactivity to naturalistic speech in sighted compared with blind subjects. The blind subjects exhibited less left lateralization to speech sounds than sighted subjects. Study III showed that early-blind people have larger spatial variability than sighted subjects in a functional auditory and parietal network, but less variability in an occipital network. Moreover, unpublished data reported here suggested that larger functional variability of the primary auditory cortex in blind subjects led to weaker activation of the auditory cortex in the blind than in sighted subjects. Study IV revealed that TMS stimulation of the prefrontal end of DTI-informed tracts between MFG and S1 impaired tactile temporal processing. Even in the PFC, an area with high inter-subject spatial variability, TMS combined with DTI and tractography revealed functional subnetworks. Thus, TMS combined with DTI and tractography can reveal neural mechanisms despite large inter-subject spatial variability.

8. Suggestions for further work

Both studies I and II suggested that many auditory areas reacted more vigorously to speech than non-speech sounds. It would be interesting to know whether stronger reactivity to speech than non-speech sounds is a general attribute of auditory areas. In Studies I and II, the speech sounds might have evoked more reliable responses in auditory areas because the stimulus included louder speech sounds than non-speech sounds. The stimulus could be improved by controlling the attributes and ratio of the speech and non-speech sounds so that the reactivity to these sounds could be directly compared.

In Study III, it was proposed that the variability of functional networks is proportional to the degree of experience-dependent plasticity driven by the sense normally attributed to the network. Whether this is a general attribute of experience-dependent plasticity could be easily verified. I expect that the auditory cortices of deaf subjects display little spatial inter-subject variability while their occipital lobe networks might show large variability. An increased regional homogeneity occurs in the occipital cortex of blind subjects (Liu et al., 2011). Whether the difference in regional homogeneity explains the differences in inter-subject spatial variability could be addressed by measuring regional homogeneity of ICA-derived functional networks (Paakki et al., 2010).

The spatial variability differences could explain differences in auditory cortex responses, not only in the blind subjects, but also among sighted subjects. As there are many large depositories with good quality fMRI data, it should be rather easy to verify or reject this hypothesis. In data sets containing resting-state and task data, the resting-state data could be used to measure inter-subject variability in networks activated in the task-condition. Next, the degree of individual variability in a specific area could be compared with the strength of the task-related responses in the same area.

Combining TMS and tractography has limitless applications. For instance, it would be interesting to explore the role of the S1-SFG link. Additionally, since DTI studies have revealed interesting changes in blind subjects anatomy (Shu et al., 2009; Yu et al., 2007), TMS-DTI studies could reveal the functional roles of these anatomical changes.

Acknowledgements

While I was working on this thesis my affiliations were the Brain Research Unit, O. V. Lounasmaa laboratory, Aalto University, and the Neuroscience Unit, Institute of Biomedicine, Helsinki University. I want to thank the directors of these institutes Pertti Hakonen and Eero Mervaala, respectively. The MRI measurements were conducted in the AMI Centre at the Aalto University. The TMS measurements were done in the BioMag laboratory TMS facilities, HUS Medical Imaging Center in the Helsinki University Central Hospital. The Academy of Finland, the aivoAALTO project, the European Research Council, the Sigrid Jusélius Foundation, and the Päivikki and Sakari Sohlberg Foundation supported the studies financially.

I wrote this thesis under the supervision of Professor Synnöve Carlson. Without her calm guidance, my restless soul would have wandered off before finishing the first draft of the first study. I am indebted to Professor Riitta Hari, the head of the Brain Research Unit, for substantial contributions to the scientific work presented here and my salary. Professor Antti Pertovaara, your passion for science and good humor is inspiring. I am also most grateful to my other coauthors; Pia Tikka, Sanna Malinen, Petri Savolainen, Juha Gogulski, Jessica Guzman and especially Mika Seppä. Without you, the thesis path would have been a rocky dead-end trail. The technical director of AMI center, Toni Auranen, and the head of the BioMag laboratory Jyrki Mäkelä provided excellent research facilities. I used to consider writing a torment; however, Caroll Norris and Ilkka Linnankoski showed me that writing is not a dreadful grammatical exercise, but a fun game. Cathy Nagini edited this thesis to the readable format before you. All remaining mistakes are of course mine alone. Liisa Peltonen and Kaj Karlstedt, I am grateful that you taught me a lot about teaching. Marita Kattelus and Anne Simola, you are the grease in the cogwheels. I'm gratefull for the improvements suggested by the thesis reviewers.

Michi, you are the only one who listened to my most absurd opinions without scorn. Virve, Ping, Chen, Maksym, Aino, Moona, Boriss, you've made the Biomedicum lab what Viljami, Lauri, Fariba, Silvia, Elyana, and the aivoAALTO posse made Otaniemi; a happy place. I cherish the multidisciplinary conversations shared with Tomas, Alexis, Wille, Okko and others. Scouting with Kasper, Daniel and the Ekenäs boys made me a decent and well-mannered man. Elina, Eino, Sini, Marja and Janne thank you for assisting me in practicalities and for setting an example. Sometimes I turned up late or left work early because the waves were breaking! Atte, Tuomas and other surfers, thank you for being my partners in crime. I wish to thank all the subjects studied for this thesis, including one who needed an excuse to leave home and participated on the 26 of December.

Mother you are my role model, and I hope my efforts make you proud. Father, you are the paragon of knowledge, please continue as my personal encyclopedia. Georg, your endeavors with electronics, computers, music, photography, humanities and politics baffle me; I wish I could be as versatile. I also want to thank my wife's family Ritva, Markku, Tytti, Kaius, Annika, and Janne for helping Tuuli and me. Selma and Leon you are my inspiration. Tuuli, you are more than words. Finally, I must acknowledge my most important teacher; my deceased dog Snowsett Chocolate Full O'Nuts. During our long strolls, I could not escape the dreadfully dull endeavor of thinking.

References

Abou-Elseoud A, Starck T, Remes J, Nikkinen J, Tervonen O, Kiviniemi V (2010) The effect of model order selection in group PICA. *Human Brain Mapping* **31:** 1207–1216

Allen EA, Damaraju E, Plis SM, Erhardt EB, Eichele T, Calhoun VD (2014) Tracking whole-brain connectivity dynamics in the resting state. *Cereb Cortex* **24:** 663–676

Allen EA, Erhardt EB, Wei Y, Eichele T, Calhoun VD (2012) Capturing inter-subject variability with group independent component analysis of fMRI data: a simulation study. *Neuroimage* **59:** 4141–4159

Amedi A, Raz N, Pianka P, Malach R, Zohary E (2003) Early 'visual'cortex activation correlates with superior verbal memory performance in the blind. *Nature neuroscience* **6:** 758–766

Amunts K, Malikovic A, Mohlberg H, Schormann T, Zilles K (2000) Brodmann's areas 17 and 18 brought into stereotaxic space-where and how variable? *Neuroimage* **11:** 66–84

Anderson SR (2004) How many languages are there in the world? *Washington, DC: Linguistic Society of America*

Arshavsky VY, Lamb TD, Pugh Jr EN (2002) G proteins and phototransduction. *Annual review of Physiology* **64:** 153–187

Bartels A, Zeki S (2004) Functional brain mapping during free viewing of natural scenes. *Hum Brain Mapp* **21:** 75–85

Bartels A, Zeki S (2005) The chronoarchitecture of the cerebral cortex. *Philos Trans R Soc Lond B Biol Sci* **360:** 733–750

Basser PJ, Mattiello J, LeBihan D (1994a) Estimation of the effective self-diffusion tensor from the NMR spin echo. *J Magn Reson B* **103:** 247–254

Basser PJ, Mattiello J, LeBihan D (1994b) MR diffusion tensor spectroscopy and imaging. *Biophys J* **66:** 259–267

Baumann O, Greenlee MW (2007) Neural correlates of coherent audiovisual motion perception. *Cereb Cortex* **17:** 1433–1443

Bavelier D, Neville HJ (2002) Cross-modal plasticity: where and how? *Nat Rev Neurosci* **3:** 443–452

Bear MF, Connors BW, Paradiso MA (2001) *Neuroscience : exploring the brain*, 2. edn. Baltimore, Md.: Lippincott Williams & Wilkins.

Behrens TE, Johansen-Berg H, Woolrich MW, Smith SM, Wheeler-Kingshott CA, Boulby PA, Barker GJ, Sillery EL, Sheehan K, Ciccarelli O, Thompson AJ, Brady JM, Matthews PM (2003a) Non-invasive mapping of connections between human thalamus and cortex using diffusion imaging. *Nat Neurosci* **6:** 750–757

Behrens TE, Woolrich MW, Jenkinson M, Johansen-Berg H, Nunes RG, Clare S, Matthews PM, Brady JM, Smith SM (2003b) Characterization and propagation of uncertainty in diffusion-weighted MR imaging. *Magn Reson Med* **50:** 1077–1088

Bijsterbosch JD, Barker AT, Lee KH, Woodruff PW (2012) Where does transcranial magnetic stimulation (TMS) stimulate? Modelling of induced field maps for some common cortical and cerebellar targets. *Med Biol Eng Comput* **50:** 671–681

Binder JR, Swanson SJ, Hammeke TA, Morris GL, Mueller WM, Fischer M, Benbadis S, Frost JA, Rao SM, Haughton VM (1996) Determination of language dominance using functional MRI: a comparison with the Wada test. *Neurology* **46:** 978–984

Biswal B, Yetkin FZ, Haughton VM, Hyde JS (1995) Functional connectivity in the motor cortex of resting human brain using echo-planar MRI. *Magn Reson Med* **34:** 537–541

Bloch F (1946) Nuclear induction. *Physical Review* **70:** 460

Bohrn IC, Altmann U, Jacobs AM (2012) Looking at the brains behind figurative language--a quantitative meta-analysis of neuroimaging studies on metaphor, idiom, and irony processing. *Neuropsychologia* **50:** 2669–2683

Boldt R, Malinen S, Seppä M, Tikka P, Savolainen P, Hari R, Carlson S (2013) Listening to an audio drama activates two processing networks, one for all sounds, another exclusively for speech. *PLoS One* **8:** e64489

Bona S, Herbert A, Toneatto C, Silvanto J, Cattaneo Z (2014) The causal role of the lateral occipital complex in visual mirror symmetry detection and grouping: an fMRI-guided TMS study. *Cortex* **51:** 46–55

Brennan J, Nir Y, Hasson U, Malach R, Heeger DJ, Pylkkänen L (2012) Syntactic structure building in the anterior temporal lobe during natural story listening. *Brain Lang* **120:** 163–173

Brett M, Johnsrude IS, Owen AM (2002) The problem of functional localization in the human brain. *Nat Rev Neurosci* **3:** 243–249

Brodmann K (2007) *Brodmann's: Localisation in the Cerebral Cortex. Translated and edited by L.J. Garey.*: Springer.

Brun CC, Leporé N, Pennec X, Lee AD, Barysheva M, Madsen SK, Avedissian C, Chou YY, de Zubicaray GI, McMahon KL, Wright MJ, Toga AW, Thompson PM (2009) Mapping the regional influence of genetics on brain structure variability--a tensor-based morphometry study. *Neuroimage* **48:** 37–49

Burton H, Diamond JB, McDermott KB (2003) Dissociating cortical regions activated by semantic and phonological tasks: a FMRI study in blind and sighted people. *J Neurophysiol* **90:** 1965–1982

Burton H, Snyder AZ, Conturo TE, Akbudak E, Ollinger JM, Raichle ME (2002a) Adaptive changes in early and late blind: a fMRI study of Braille reading. *J Neurophysiol* **87:** 589–607

Burton H, Snyder AZ, Diamond JB, Raichle ME (2002b) Adaptive changes in early and late blind: a FMRI study of verb generation to heard nouns. *J Neurophysiol* **88:** 3359–3371

Calhoun VD, Adali T (2006) Unmixing fMRI with independent component analysis. *IEEE Eng Med Biol Mag* **25:** 79–90

Calhoun VD, Adali T (2012) Multisubject independent component analysis of fMRI: a decade of intrinsic networks, default mode, and neurodiagnostic discovery. *IEEE Rev Biomed Eng* **5:** 60–73

Calhoun VD, Adali T, Pearlson GD, Pekar JJ (2001) A method for making group inferences from functional MRI data using independent component analysis. *Hum Brain Mapp* **14:** 140–151

Calvert GA, Hansen PC, Iversen SD, Brammer MJ (2001) Detection of audio-visual integration sites in humans by application of electrophysiological criteria to the BOLD effect. *Neuroimage* **14:** 427–438

Carlson S, Rama P, Tanila H, Linnankoski I, Mansikka H (1997) Dissociation of mnemonic coding and other functional neuronal processing in the monkey prefrontal cortex. *Journal of Neurophysiology* **77:** 761–774

Catani M, Howard RJ, Pajevic S, Jones DK (2002) Virtual in Vivo Interactive Dissection of White Matter Fasciculi in the Human Brain. *Neuroimage* **17:** 77–94

Cauda F, D'Agata F, Sacco K, Duca S, Geminiani G, Vercelli A (2011) Functional connectivity of the insula in the resting brain. *Neuroimage* **55:** 8–23

Chao LL, Knight RT (1995) Human prefrontal lesions increase distractibility to irrelevant sensory inputs. *Neuroreport* **6:** 1605–1610

Christoff K, Gordon AM, Smallwood J, Smith R, Schooler JW (2009) Experience sampling during fMRI reveals default network and executive system contributions to mind wandering. *Proceedings of the National Academy of Sciences* **106:** 8719–8724

Ciccarelli O, Behrens TE, Altmann DR, Orrell RW, Howard RS, Johansen-Berg H, Miller DH, Matthews PM, Thompson AJ (2006) Probabilistic diffusion tractography: a potential tool to assess the rate of disease progression in amyotrophic lateral sclerosis. *Brain* **129:** 1859–1871

Cohen LG, Celnik P, Pascual-Leone A, Corwell B, Faiz L, Dambrosia J, Honda M, Sadato N, Gerloff C, Catala MD (1997) Functional relevance of cross-modal plasticity in blind humans. *Nature* **389:** 180–183

Conroy BR, Singer BD, Guntupalli JS, Ramadge PJ, Haxby JV (2013) Inter-subject alignment of human cortical anatomy using functional connectivity. *Neuroimage* **81:** 400–411

Cowey A (2005) The Ferrier Lecture 2004 what can transcranial magnetic stimulation tell us about how the brain works? *Philos Trans R Soc Lond B Biol Sci* **360:** 1185–1205

Damadian R (1971) Tumor detection by nuclear magnetic resonance. *Science* **171:** 1151–1153

Damasio H, Grabowski T, Frank R, Galaburda AM, Damasio AR (1994) The return of Phineas Gage: clues about the brain from the skull of a famous patient. *Science* **264:** 1102–1105

Damoiseaux JS, Rombouts SA, Barkhof F, Scheltens P, Stam CJ, Smith SM, Beckmann CF (2006) Consistent resting-state networks across healthy subjects. *Proc Natl Acad Sci U S A* **103:** 13848–13853

Daniel P, Whitteridge D (1961) The representation of the visual field on the cerebral cortex in monkeys. *The Journal of physiology* **159:** 203–221

Deco G, Jirsa VK, McIntosh AR (2011) Emerging concepts for the dynamical organization of resting-state activity in the brain. *Nat Rev Neurosci* **12:** 43–56

Di X, Gohel S, Kim EH, Biswal BB (2013) Task vs. rest-different network configurations between the coactivation and the resting-state brain networks. *Front Hum Neurosci* **7:** 493

Draganski B, Gaser C, Busch V, Schuierer G, Bogdahn U, May A (2004) Neuroplasticity: Changes in grey matter induced by training. *Nature* **427:** 311–312

Du Y, Fan Y (2013) Group information guided ICA for fMRI data analysis. *Neuroimage* **69:** 157–197

Dym RJ, Burns J, Freeman K, Lipton ML (2011) Is functional MR imaging assessment of hemispheric language dominance as good as the Wada test?: a meta-analysis. *Radiology* **261:** 446–455

Eickhoff SB, Stephan KE, Mohlberg H, Grefkes C, Fink GR, Amunts K, Zilles K (2005) A new SPM toolbox for combining probabilistic cytoarchitectonic maps and functional imaging data. *Neuroimage* **25:** 1325–1335

Einstein A (1905) On the movement of small particles suspended in stationary liquids required by the molecular-kinetic theory of heat. *Annalen der Physik* **17:** 16

Elbert T, Pantev C, Wienbruch C, Rockstroh B, Taub E (1995) Increased cortical representation of the fingers of the left hand in string players. *Science* **270:** 305–307

Elbert T, Sterr A, Rockstroh B, Pantev C, Müller MM, Taub E (2002) Expansion of the tonotopic area in the auditory cortex of the blind. *The Journal of Neuroscience* **22:** 9941–9944

Elston GN, Oga T, Fujita I (2009) Spinogenesis and pruning scales across functional hierarchies. *J Neurosci* **29:** 3271–3275

Erhardt EB, Rachakonda S, Bedrick EJ, Allen EA, Adali T, Calhoun VD (2011) Comparison of multi-subject ICA methods for analysis of fMRI data. *Hum Brain Mapp* **32:** 2075–2095

Fagiolini M, Hensch TK (2000) Inhibitory threshold for critical-period activation in primary visual cortex. *Nature* **404:** 183–186

Fair DA, Cohen AL, Power JD, Dosenbach NU, Church JA, Miezin FM, Schlaggar BL, Petersen SE (2009) Functional brain networks develop from a "local to distributed" organization. *PLoS Comput Biol* **5:** e1000381

Farivar R (2009) Dorsal–ventral integration in object recognition. *Brain Research Reviews* **61:** 144–153

Felleman DJ, Van Essen DC (1991) Distributed hierarchical processing in the primate cerebral cortex. *Cerebral Cortex* **1:** 1–47

Fitzgerald PB, Fountain S, Daskalakis ZJ (2006) A comprehensive review of the effects of rTMS on motor cortical excitability and inhibition. *Clinical Neurophysiology* **117:** 2584–2596

Formisano E, De Martino F, Bonte M, Goebel R (2008) "Who" is saying "what"? Brain-based decoding of human voice and speech. *Science* **322:** 970–973

Fransson P, Skiöld B, Horsch S, Nordell A, Blennow M, Lagercrantz H, Aden U (2007) Resting-state networks in the infant brain. *Proc Natl Acad Sci U S A* **104:** 15531–15536

Friston K, Jezzard P, Turner R (1994) Analysis of functional MRI time-series. *Human Brain Mapping* **1:** 153–171

Frost MA, Esposito F, Goebel R (2014) Improved correspondence of resting-state networks after macroanatomical alignment. *Hum Brain Mapp* **35:** 673–682

Frost MA, Goebel R (2012) Measuring structural-functional correspondence: spatial variability of specialised brain regions after macro-anatomical alignment. *Neuroimage* **59:** 1369–1381

Geschwind N (1970) The organization of language and the brain.

Geschwind N, Levitsky W (1968) Human brain: left-right asymmetries in temporal speech region. *Science* **161:** 186–187

Giraud AL, Kleinschmidt A, Poeppel D, Lund TE, Frackowiak RS, Laufs H (2007) Endogenous cortical rhythms determine cerebral specialization for speech perception and production. *Neuron* **56:** 1127–1134

Glahn DC, Winkler AM, Kochunov P, Almasy L, Duggirala R, Carless MA, Curran JC, Olvera RL, Laird AR, Smith SM, Beckmann CF, Fox PT, Blangero J (2010) Genetic control over the resting brain. *Proc Natl Acad Sci U S A* **107:** 1223–1228

Gogulski J, Boldt R, Savolainen P, Guzmán-López J, Carlson S, Pertovaara A (2013) A Segregated Neural Pathway for Prefrontal Top-Down Control of Tactile Discrimination. *Cereb Cortex***:** 2013 Aug 2019. [Epub ahead of print]

Golland Y, Golland P, Bentin S, Malach R (2008) Data-driven clustering reveals a fundamental subdivision of the human cortex into two global systems. *Neuropsychologia* **46:** 540–553

Goodale MA, Milner AD (1992) Separate visual pathways for perception and action. *Trends Neurosci* **15:** 20–25

Goodman CS, Shatz CJ (1993) Developmental mechanisms that generate precise patterns of neuronal connectivity. *Cell* **72 Suppl:** 77–98

Gori M, Sandini G, Martinoli C, Burr DC (2014) Impairment of auditory spatial localization in congenitally blind human subjects. *Brain* **137:** 288–293

Gougoux F, Belin P, Voss P, Lepore F, Lassonde M, Zatorre RJ (2009) Voice perception in blind persons: a functional magnetic resonance imaging study. *Neuropsychologia* **47:** 2967–2974

Greicius MD, Kiviniemi V, Tervonen O, Vainionpää V, Alahuhta S, Reiss AL, Menon V (2008) Persistent default-mode network connectivity during light sedation. *Human Brain Mapping* **29:** 839–847

Greicius MD, Srivastava G, Reiss AL, Menon V (2004) Default-mode network activity distinguishes Alzheimer's disease from healthy aging: evidence from functional MRI. *Proc Natl Acad Sci U S A* **101:** 4637–4642

Greicius MD, Supekar K, Menon V, Dougherty RF (2009) Resting-state functional connectivity reflects structural connectivity in the default mode network. *Cerebral Cortex* **19:** 72–78

Günter E (2006) *Hemisphere Dominance of Brain Function-Which Functions Are Lateralized and Why? In: 23 Problems in Systems Neuroscience*: Oxford University Press.

Hallett M (2000) Transcranial magnetic stimulation and the human brain. *Nature* **406:** 147–150

Hannula H, Neuvonen T, Savolainen P, Hiltunen J, Ma YY, Antila H, Salonen O, Carlson S, Pertovaara A (2010) Increasing top-down suppression from prefrontal cortex facilitates tactile working memory. *Neuroimage* **49:** 1091–1098

Hannula H, Ylioja S, Pertovaara A, Korvenoja A, Ruohonen J, Ilmoniemi RJ, Carlson S (2005) Somatotopic blocking of sensation with navigated transcranial magnetic stimulation of the primary somatosensory cortex. *Hum Brain Mapp* **26:** 100–109

Hasson U, Nir Y, Levy I, Fuhrmann G, Malach R (2004) Intersubject synchronization of cortical activity during natural vision. *Science* **303:** 1634–1640

Held R, Ostrovsky Y, de Gelder B, Gandhi T, Ganesh S, Mathur U, Sinha P (2011) The newly sighted fail to match seen with felt. *Nature neuroscience* **14:** 551–553

Hensch TK (2005) Critical period plasticity in local cortical circuits. *Nature Reviews Neuroscience* **6:** 877–888

Herdener M, Esposito F, Di Salle F, Boller C, Hilti CC, Habermeyer B, Scheffler K, Wetzel S, Seifritz E, Cattapan-Ludewig K (2010) Musical training induces functional plasticity in human hippocampus. *The Journal of Neuroscience* **30:** 1377–1384

Hickok G, Poeppel D (2007) The cortical organization of speech processing. *Nat Rev Neurosci* **8:** 393–402

Himberg J, Hyvärinen A, Esposito F (2004) Validating the independent components of neuroimaging time series via clustering and visualization. *Neuroimage* **22:** 1214–1222

Honey C, Sporns O, Cammoun L, Gigandet X, Thiran J-P, Meuli R, Hagmann P (2009) Predicting human resting-state functional connectivity from structural connectivity. *Proceedings of the National Academy of Sciences* **106:** 2035–2040

Hubel DH, Wiesel TN (1959) Receptive fields of single neurones in the cat's striate cortex. *The Journal of physiology* **148:** 574

Hubel DH, Wiesel TN (1963) Receptive fields of cells in striate cortex of very young, visually inexperienced kittens. *J Neurophysiol* **26:** 994–1002

Hudspeth A (1997) How hearing happens. *Neuron* **19:** 947–950

Hudspeth AJ (1989) How the ear's works work. *Nature* **341:** 397–404

Huettel SA, Song AW, McCarthy G (2004) *Functional magnetic resonance imaging*, Sunderland, Mass.: Sinauer Associates.

Jafri MJ, Pearlson GD, Stevens M, Calhoun VD (2008) A method for functional network connectivity among spatially independent resting-state components in schizophrenia. *Neuroimage* **39:** 1666–1681

Jamadar S, Powers NR, Meda SA, Calhoun VD, Gelernter J, Gruen JR, Pearlson GD (2013) Genetic influences of resting state fMRI activity in language-related brain regions in healthy controls and schizophrenia patients: a pilot study. *Brain Imaging Behav* **7:** 15–27

Jang JH, Jung WH, Kang DH, Byun MS, Kwon SJ, Choi CH, Kwon JS (2011) Increased default mode network connectivity associated with meditation. *Neurosci Lett* **487:** 358–362

Jenkins WM, Merzenich MM, Ochs MT, Allard T, Guíc-Robles E (1990) Functional reorganization of primary somatosensory cortex in adult owl monkeys after behaviorally controlled tactile stimulation. *J Neurophysiol* **63:** 82–104

Jiang J, Zhu W, Shi F, Liu Y, Li J, Qin W, Li K, Yu C, Jiang T (2009) Thick visual cortex in the early blind. *J Neurosci* **29:** 2205–2211

Joel SE, Caffo BS, van Zijl PC, Pekar JJ (2011) On the relationship between seed-based and ICA-based measures of functional connectivity. *Magn Reson Med* **66:** 644–657

Jones DK. (2010) Diffusion MRI--Theory, Methods, and Applications. Oxford University Press, USA, Oxford.

Karni A, Meyer G, Jezzard P, Adams MM, Turner R, Ungerleider LG (1995) Functional MRI evidence for adult motor cortex plasticity during motor skill learning. *Nature* **377:** 155–158

Karni A, Meyer G, Rey-Hipolito C, Jezzard P, Adams MM, Turner R, Ungerleider LG (1998) The acquisition of skilled motor performance: fast and slow experience-driven changes in primary motor cortex. *Proceedings of the National Academy of Sciences* **95:** 861–868

Kiviniemi V, Kantola J, Jauhiainen J, Hyvarinen A, Tervonen O (2003) Independent component analysis of nondeterministic fMRI signal sources. *Neuroimage* **19:** 253–260

Koelsch S (2011) Toward a neural basis of music perception - a review and updated model. *Frontiers in psychology* **2:** 110

Koelsch S, Gunter TC, v Cramon DY, Zysset S, Lohmann G, Friederici AD (2002) Bach speaks: a cortical "language-network" serves the processing of music. *Neuroimage* **17:** 956–966

Kriegeskorte N, Simmons WK, Bellgowan PS, Baker CI (2009) Circular analysis in systems neuroscience: the dangers of double dipping. *Nat Neurosci* **12:** 535–540

Kätsyri J, Hari R, Ravaja N, Nummenmaa L (2013) The opponent matters: elevated FMRI reward responses to winning against a human versus a computer opponent during interactive video game playing. *Cereb Cortex* **23:** 2829–2839

Lahnakoski JM, Salmi J, Jääskeläinen IP, Lampinen J, Glerean E, Tikka P, Sams M (2012) Stimulus-related independent component and voxel-wise analysis of human brain activity during free viewing of a feature film. *PLoS One* **7:** e35215

Lankinen K, Saari J, Hari R, Koskinen M (2014) Intersubject consistency of cortical MEG signals during movie viewing. *Neuroimage* **92C:** 217–224

Lauterbur PC (1973) Image formation by induced local interactions: examples employing nuclear magnetic resonance. *Nature* **242:** 190–191

Lawes INC, Barrick TR, Murugam V, Spierings N, Evans DR, Song M, Clark CA (2008) Atlas-based segmentation of white matter tracts of the human brain using diffusion tensor tractography and comparison with classical dissection. *Neuroimage* **39:** 62–79

Lee MH, Hacker CD, Snyder AZ, Corbetta M, Zhang D, Leuthardt EC, Shimony JS (2012) Clustering of resting state networks. *PLoS One* **7:** e40370

Lee TW, Girolami M, Sejnowski TJ (1999) Independent component analysis using an extended infomax algorithm for mixed subgaussian and supergaussian sources. *Neural Computation* **11:** 417–441

Lefaucheur J-P (2009) Methods of therapeutic cortical stimulation. *Neurophysiologie Clinique/Clinical Neurophysiology* **39:** 1–14

Lerner Y, Honey CJ, Silbert LJ, Hasson U (2011) Topographic mapping of a hierarchy of temporal receptive windows using a narrated story. *J Neurosci* **31:** 2906–2915

Lessard N, Paré M, Lepore F, Lassonde M (1998) Early-blind human subjects localize sound sources better than sighted subjects. *Nature* **395:** 278–280

Lewis JW, Wightman FL, Brefczynski JA, Phinney RE, Binder JR, DeYoe EA (2004) Human brain regions involved in recognizing environmental sounds. *Cereb Cortex* **14:** 1008–1021

Li YO, Adali T, Calhoun VD (2007) Estimating the number of independent components for functional magnetic resonance imaging data. *Hum Brain Mapp* **28:** 1251–1266

Liberman AM, Mattingly IG (1985) The motor theory of speech perception revised. *Cognition* **21:** 1–36

Lin FH, Wald LL, Ahlfors SP, Hämäläinen MS, Kwong KK, Belliveau JW (2006) Dynamic magnetic resonance inverse imaging of human brain function. *Magnetic resonance in medicine* **56:** 787–802

Littow H, Elseoud AA, Haapea M, Isohanni M, Moilanen I, Mankinen K, Nikkinen J, Rahko J, Rantala H, Remes J (2010) Age-related differences in functional nodes of the brain cortex–a high model order group ICA study. *Frontiers in systems neuroscience* **4:** 32

Liu C, Liu Y, Li W, Wang D, Jiang T, Zhang Y, Yu C (2011) Increased regional homogeneity of blood oxygen level-dependent signals in occipital cortex of early blind individuals. *Neuroreport* **22:** 190–194

Liu Y, Yu C, Liang M, Li J, Tian L, Zhou Y, Qin W, Li K, Jiang T (2007) Whole brain functional connectivity in the early blind. *Brain* **130:** 2085–2096

Locke J (1700) *An essay concerning human understanding*.

Logothetis NK (2003) The underpinnings of the BOLD functional magnetic resonance imaging signal. *The Journal of Neuroscience* **23:** 3963–3971

Logothetis NK (2008) What we can do and what we cannot do with fMRI. *Nature* **453:** 869–878

Logothetis NK, Pauls J, Augath M, Trinath T, Oeltermann A (2001) Neurophysiological investigation of the basis of the fMRI signal. *Nature* **412:** 150–157

Luo H, Poeppel D (2007) Phase patterns of neuronal responses reliably discriminate speech in human auditory cortex. *Neuron* **54:** 1001–1010

Maguire EA, Gadian DG, Johnsrude IS, Good CD, Ashburner J, Frackowiak RS, Frith CD (2000) Navigation-related structural change in the hippocampi of taxi drivers. *Proceedings of the National Academy of Sciences* **97:** 4398–4403

Malikovic A, Amunts K, Schleicher A, Mohlberg H, Eickhoff SB, Wilms M, Palomero-Gallagher N, Armstrong E, Zilles K (2007) Cytoarchitectonic analysis of the human extrastriate cortex in the region of V5/MT+: a probabilistic, stereotaxic map of area hOc5. *Cereb Cortex* **17:** 562–574

Malinen S, Hari R (2011) Data-based functional template for sorting independent components of fMRI activity. *Neurosci Res* **71:** 369–376

Malinen S, Hlushchuk Y, Hari R (2007) Towards natural stimulation in fMRI--issues of data analysis. *Neuroimage* **35:** 131–139

Mansfield P (1977) Multi-planar image formation using NMR spin echoes. *Journal of Physics C: Solid State Physics* **10:** L55

Mansfield P, Maudsley A (1976) Planar spin imaging by NMR. *Journal of Physics C: Solid State Physics* **9:** L409

McKeown MJ, Jung T-P, Makeig S, Brown G, Kindermann SS, Lee T-W, Sejnowski TJ (1998) Spatially independent activity patterns in functional MRI data during the Stroop color-naming task. *Proceedings of the National Academy of Sciences* **95:** 803–810

McKeown MJ, Makeig S, Brown GG, Jung T-P, Kindermann SS, Bell AJ, Sejnowski TJ. (1997) Analysis of fMRI data by blind separation into independent spatial components. *Hum Brain Mapping* **6**: 160–88.

McKeown MJ, Sejnowski TJ (1998) Independent component analysis of fMRI data: examining the assumptions. *Human Brain Mapping* **6:** 368–372

Merzenich MM, Brugge JF (1973) Representation of the cochlear partition of the superior temporal plane of the macaque monkey. *Brain Res* **50:** 275–296

Merzenich MM, Nelson RJ, Stryker MP, Cynader MS, Schoppmann A, Zook JM (1984) Somatosensory cortical map changes following digit amputation in adult monkeys. *J Comp Neurol* **224:** 591–605

Milner AD, Goodale MA (2008) Two visual systems re-viewed. *Neuropsychologia* **46:** 774–785

Moerel M, De Martino F, Formisano E (2012) Processing of natural sounds in human auditory cortex: tonotopy, spectral tuning, and relation to voice sensitivity. *J Neurosci* **32:** 14205–14216

Montague PR, Berns GS, Cohen JD, McClure SM, Pagnoni G, Dhamala M, Wiest MC, Karpov I, King RD, Apple N, Fisher RE (2002) Hyperscanning: simultaneous fMRI during linked social interactions. *Neuroimage* **16:** 1159–1164

Morosan P, Rademacher J, Schleicher A, Amunts K, Schormann T, Zilles K (2001) Human primary auditory cortex: cytoarchitectonic subdivisions and mapping into a spatial reference system. *Neuroimage* **13:** 684–701

Morosan P, Schleicher A, Amunts K, Zilles K (2005) Multimodal architectonic mapping of human superior temporal gyrus. *Anat Embryol (Berl)* **210:** 401–406

Mueller S, Wang D, Fox MD, Yeo BT, Sepulcre J, Sabuncu MR, Shafee R, Lu J, Liu H (2013) Individual variability in functional connectivity architecture of the human brain. *Neuron* **77:** 586–595

Nath AR, Beauchamp MS (2012) A neural basis for interindividual differences in the McGurk effect, a multisensory speech illusion. *Neuroimage* **59:** 781–787

Nava E, Güntürkün O, Röder B (2013) Experience-dependent emergence of functional asymmetries. *Laterality* **18:** 407–415

Nobelprize.org. The Nobel Prize in Physics 1944.

Nobelprize.org. The Nobel Prize in Physics 1952.

Nobelprize.org. The Nobel Prize in Physiology or Medicine 1981.

Nobelprize.org. The Nobel Prize in Physiology or Medicine 2003.

Nummenmaa A, McNab JA, Savadjiev P, Okada Y, Hämäläinen MS, Wang R, Wald LL, Pascual-Leone A, Wedeen VJ, Raij T (2014) Targeting of white matter tracts with transcranial magnetic stimulation. *Brain Stimul* **7:** 80–84

Nummenmaa L, Glerean E, Viinikainen M, Jaaskelainen I, Hari R, Sams M (2012) Emotions promote social interaction by synchronizing brain activity across individuals. *Proc Natl Acad Sci U S A* **109:** 9599–9604

Nurminen L (2013) Spatial context in the early visual system.

Obleser J, Wise RJ, Dresner MA, Scott SK (2007) Functional integration across brain regions improves speech perception under adverse listening conditions. *The Journal of Neuroscience* **27:** 2283–2289

Ogawa S, Lee T, Kay A, Tank D (1990) Brain magnetic resonance imaging with contrast dependent on blood oxygenation. *Proceedings of the National Academy of Sciences* **87:** 9868–9872

Ogawa S, Tank DW, Menon R, Ellermann JM, Kim SG, Merkle H, Ugurbil K (1992) Intrinsic signal changes accompanying sensory stimulation: functional brain mapping with magnetic resonance imaging. *Proceedings of the National Academy of Sciences* **89:** 5951–5955

Paakki J-J, Rahko J, Long X, Moilanen I, Tervonen O, Nikkinen J, Starck T, Remes J, Hurtig T, Haapsamo H (2010) Alterations in regional homogeneity of resting-state brain activity in autism spectrum disorders. *Brain Res* **1321:** 169–179

Park H-J, Lee JD, Kim EY, Park B, Oh M-K, Lee S, Kim J-J (2009) Morphological alterations in the congenital blind based on the analysis of cortical thickness and surface area. *Neuroimage* **47:** 98–106

Pascual-Leone A, Amedi A, Fregni F, Merabet LB (2005) The plastic human brain cortex. *Annu Rev Neurosci* **28:** 377–401

Pascual-Leone A, Torres F (1993) Plasticity of the sensorimotor cortex representation of the reading finger in Braille readers. *Brain* **116:** 39–52

Pastor MA, Day BL, Macaluso E, Friston KJ, Frackowiak RS (2004) The functional neuroanatomy of temporal discrimination. *J Neurosci* **24:** 2585–2591

Poeppel D, Emmorey K, Hickok G, Pylkkänen L (2012) Towards a new neurobiology of language. *The Journal of Neuroscience* **32:** 14125–14131

Pons TP, Garraghty PE, Ommaya AK, Kaas JH, Taub E, Mishkin M (1991) Massive cortical reorganization after sensory deafferentation in adult macaques. *Science* **252:** 1857–1860

Preuss TM, Goldman-Rakic PS (1989) Connections of the ventral granular frontal cortex of macaques with perisylvian premotor and somatosensory areas: anatomical evidence for somatic representation in primate frontal association cortex. *Journal of comparative neurology* **282:** 293–316

Raichle ME, MacLeod AM, Snyder AZ, Powers WJ, Gusnard DA, Shulman GL (2001) A default mode of brain function. *Proc Natl Acad Sci U S A* **98:** 676–682

Rapp AM, Mutschler DE, Erb M (2012) Where in the brain is nonliteral language? A coordinate-based meta-analysis of functional magnetic resonance imaging studies. *Neuroimage* **63:** 600–610

Rasmussen T, Milner B (1977) The role of early left-brain injury in determining lateralization of cerebral speech functions. *Ann N Y Acad Sci* **299:** 355–369

Rauschecker JP (2011) An expanded role for the dorsal auditory pathway in sensorimotor control and integration. *Hear Res* **271:** 16–25

Romanski LM, Tian B, Fritz J, Mishkin M, Goldman-Rakic PS, Rauschecker JP (1999) Dual streams of auditory afferents target multiple domains in the primate prefrontal cortex. *Nat Neurosci* **2:** 1131–1136

Rusconi E, Pinel P, Dehaene S, Kleinschmidt A (2010) The enigma of Gerstmann's syndrome revisited: a telling tale of the vicissitudes of neuropsychology. *Brain* **133:** 320–332

Rust NC, Movshon JA (2005) In praise of artifice. *Nat Neurosci* **8:** 1647–1650

Röder B, Rösler F, Neville HJ (2000) Event-related potentials during auditory language processing in congenitally blind and sighted people. *Neuropsychologia* **38:** 1482–1502

Röder B, Stock O, Bien S, Neville H, Rösler F (2002) Speech processing activates visual cortex in congenitally blind humans. *Eur J Neurosci* **16:** 930–936

Röder B, Teder-Sälejärvi W, Sterr A, Rösler F, Hillyard SA, Neville HJ (1999) Improved auditory spatial tuning in blind humans. *Nature* **400:** 162–166

Sadato N, Okada T, Honda M, Yonekura Y (2002) Critical period for cross-modal plasticity in blind humans: a functional MRI study. *Neuroimage* **16:** 389–400

Sadato N, Pascual-Leone A, Grafman J, Deiber MP, Ibañez V, Hallett M (1998) Neural networks for Braille reading by the blind. *Brain* **121 (Pt 7):** 1213–1229

Sams M, Aulanko R, Hämäläinen M, Hari R, Lounasmaa OV, Lu ST, Simola J (1991) Seeing speech: visual information from lip movements modifies activity in the human auditory cortex. *Neurosci Lett* **127:** 141–145

Satterthwaite TD, Wolf DH, Ruparel K, Erus G, Elliott MA, Eickhoff SB, Gennatas ED, Jackson C, Prabhakaran K, Smith A, Hakonarson H, Verma R, Davatzikos C, Gur RE, Gur RC (2013) Heterogeneous impact of motion on fundamental patterns of developmental changes in functional connectivity during youth. *Neuroimage* **83C:** 45–57

Savolainen P, Carlson S, Boldt R, Neuvonen T, Hannula H, Hiltunen J, Salonen O, Ma YY, Pertovaara A (2011) Facilitation of tactile working memory by top-down suppression from prefrontal to primary somatosensory cortex during sensory interference. *Behav Brain Res* **219:** 387–390

Schmithorst VJ, Holland SK, Plante E (2006) Cognitive modules utilized for narrative comprehension in children: A functional magnetic resonance imaging study. *Neuroimage* **29:** 254–266

Schwanenflugel PJ, Shoben EJ (1985) The influence of sentence constraint on the scope of facilitation for upcoming words. *Journal of Memory and Language* **24:** 232–252

Segal E, Petrides M (2013) Functional activation during reading in relation to the sulci of the angular gyrus region. *Eur J Neurosci* **38:** 2793–2801

Seghier ML (2013) The angular gyrus: multiple functions and multiple subdivisions. *Neuroscientist* **19:** 43–61

Shu N, Liu Y, Li J, Li Y, Yu C, Jiang T (2009) Altered anatomical network in early blindness revealed by diffusion tensor tractography. *PLoS One* **4:** e7228

Smith SM (2012) The future of FMRI connectivity. *Neuroimage* **62:** 1257–1266

Smith SM, Fox PT, Miller KL, Glahn DC, Fox PM, Mackay CE, Filippini N, Watkins KE, Toro R, Laird AR, Beckmann CF (2009) Correspondence of the brain's functional architecture during activation and rest. *Proc Natl Acad Sci U S A* **106:** 13040–13045

Speelman CP, McGann M (2013) How Mean is the Mean? *Front Psychol* **4:** 451

Starck T, Nissilä J, Aunio A, Abou-Elseoud A, Remes J, Nikkinen J, Timonen M, Takala T, Tervonen O, Kiviniemi V (2012) Stimulating brain tissue with bright light alters functional connectivity in brain at the resting state.

Stephens GJ, Honey CJ, Hasson U (2013) A place for time: the spatiotemporal structure of neural dynamics during natural audition. *Journal of Neurophysiology* **110:** 2019–2026

Stephens GJ, Silbert LJ, Hasson U (2010) Speaker-listener neural coupling underlies successful communication. *Proc Natl Acad Sci U S A* **107:** 14425–14430

Sterr A, Müller MM, Elbert T, Rockstroh B, Pantev C, Taub E (1998) Perceptual correlates of changes in cortical representation of fingers in blind multifinger Braille readers. *The Journal of Neuroscience* **18:** 4417–4423

Stevens MC, Kiehl KA, Pearlson G, Calhoun VD (2007) Functional neural circuits for mental timekeeping. *Hum Brain Mapp* **28:** 394–408

Striem-Amit E, Dakwar O, Reich L, Amedi A (2012) The large-scale organization of "visual" streams emerges without visual experience. *Cereb Cortex* **22:** 1698–1709

Sugiura M, Friston KJ, Willmes K, Shah NJ, Zilles K, Fink GR (2007) Analysis of intersubject variability in activation: an application to the incidental episodic retrieval during recognition test. *Hum Brain Mapp* **28:** 49–58

Swets JA (1973) The Relative Operating Characteristic in Psychology: A technique for isolating effects of response bias finds wide use in the study of perception and cognition. *Science* **182:** 990–1000

Szycik GR, Stadler J, Tempelmann C, Münte TF (2012) Examining the McGurk illusion using high-field 7 Tesla functional MRI. *Front Hum Neurosci* **6:** 95

Tervaniemi M, Hugdahl K (2003) Lateralization of auditory-cortex functions. *Brain Res Brain Res Rev* **43:** 231–246

Thompson PM, Cannon TD, Narr KL, Van Erp T, Poutanen V-P, Huttunen M, Lönnqvist J, Standertskjöld-Nordenstam C-G, Kaprio J, Khaledy M (2001) Genetic influences on brain structure. *Nature neuroscience* **4:** 1253–1258

Toga AW, Thompson PM, Mori S, Amunts K, Zilles K (2006) Towards multimodal atlases of the human brain. *Nat Rev Neurosci* **7:** 952–966

Tomaiuolo F, MacDonald JD, Caramanos Z, Posner G, Chiavaras M, Evans AC, Petrides M (1999) Morphology, morphometry and probability mapping of the pars opercularis of the inferior frontal gyrus: an in vivo MRI analysis. *Eur J Neurosci* **11:** 3033–3046

Torrey HC (1956) Bloch Equations with Diffusion Terms. *Physical Review* **104:** 3

Tortora GJ, Derrickson B (2009) *Principles of anatomy and physiology. Vol. 1, Organization, support and movement, and control systems of the human body*, 12. uppl. edn. New York: Wiley.

Tóthová J, Vasziová G, Glod L, Lisý V (2011) Langevin theory of anomalous Brownian motion made simple. *European journal of physics* **32:** 645

Ungerleider SK, Leslie G (2000) Mechanisms of visual attention in the human cortex. *Annual review of neuroscience* **23:** 315–341

Wang D, Qin W, Liu Y, Zhang Y, Jiang T, Yu C (2014) Altered resting-state network connectivity in congenital blind. *Hum Brain Mapp* **35:** 2573–2581

Wansapura JP, Holland SK, Dunn RS, Ball WS (1999) NMR relaxation times in the human brain at 3.0 tesla. *J Magn Reson Imaging* **9:** 531–538

Wasserman EM (2007) *The Oxford handbook of transcranial stimulation*, Oxford ; New York: Oxford University Press.

Watkins KE, Cowey A, Alexander I, Filippini N, Kennedy JM, Smith SM, Ragge N, Bridge H (2012) Language networks in anophthalmia: maintained hierarchy of processing in 'visual' cortex. *Brain* **135:** 1566–1577

Watkins KE, Shakespeare TJ, O'Donoghue MC, Alexander I, Ragge N, Cowey A, Bridge H (2013) Early auditory processing in area V5/MT+ of the congenitally blind brain. *J Neurosci* **33:** 18242–18246

Watkins KE, Strafella AP, Paus T (2003) Seeing and hearing speech excites the motor system involved in speech production. *Neuropsychologia* **41:** 989–994

Whittingstall K, Bartels A, Singh V, Kwon S, Logothetis NK (2010) Integration of EEG source imaging and fMRI during continuous viewing of natural movies. *Magnetic resonance imaging* **28:** 1135–1142

Wiesel T, Hubel D, Lam D (1974) Autoradiographic demonstration of ocular-dominance columns in the monkey striate cortex by means of transneuronal transport. *Brain Res* **79:** 273–279

Wiesel TN (1982) Postnatal development of the visual cortex and the influence of environment. *Nature* **299:** 583–591

Wiesel TN, Hubel DH (1963) Single-cell responses in striate cortex of kittens deprived of vision in one eye. *J Neurophysiol* **26:** 1003–1017

Wiesel TN, Hubel DH (1965a) Comparison of the effects of unilateral and bilateral eye closure on cortical unit responses in kittens. *J Neurophysiol* **28:** 1029–1040

Wiesel TN, Hubel DH (1965b) Extent of recovery from the effects of visual deprivation in kittens. *J Neurophysiol* **28:** 1060–1072

Wilke M, Lidzba K (2007) LI-tool: a new toolbox to assess lateralization in functional MR-data. *J Neurosci Methods* **163:** 128–136

Wilke M, Schmithorst VJ (2006) A combined bootstrap/histogram analysis approach for computing a lateralization index from neuroimaging data. *Neuroimage* **33:** 522–530

Wilms M, Eickhoff SB, Specht K, Amunts K, Shah NJ, Malikovic A, Fink GR (2005) Human V5/MT+: comparison of functional and cytoarchitectonic data. *Anat Embryol (Berl)* **210:** 485–495

Wilson SM, Molnar-Szakacs I, Iacoboni M (2008) Beyond superior temporal cortex: intersubject correlations in narrative speech comprehension. *Cereb Cortex* **18:** 230–242

Witelson SF, Pallie W (1973) Left hemisphere specialization for language in the newborn. Neuroanatomical evidence of asymmetry. *Brain* **96:** 641–646

Yamaguchi S, Knight R (1990) Gating of somatosensory input by human prefrontal cortex. *Brain Res* **521:** 281–288

Yu C, Shu N, Li J, Qin W, Jiang T, Li K (2007) Plasticity of the corticospinal tract in early blindness revealed by quantitative analysis of fractional anisotropy based on diffusion tensor tractography. *Neuroimage* **36:** 411–417

Zeki S, Watson J, Lueck C, Friston KJ, Kennard C, Frackowiak R (1991) A direct demonstration of functional specialization in human visual cortex. *The Journal of Neuroscience* **11:** 641–649

Zilles K, Amunts K (2010) Centenary of Brodmann's map—conception and fate. *Nature Reviews Neuroscience* **11:** 139–145

Zilles K, Amunts K (2013) Individual variability is not noise. *Trends Cogn Sci* **17:** 153–155

Zilles K, Amunts K, Smaers JB (2011) Three brain collections for comparative neuroanatomy and neuroimaging. *Ann N Y Acad Sci* **1225 Suppl 1:** E94–104

Zilles K, Schleicher A, Langemann C, Amunts K, Morosan P, Palomero-Gallagher N, Schormann T, Mohlberg H, Bürgel U, Steinmetz H, Schlaug G, Roland PE (1997) Quantitative analysis of sulci in the human cerebral cortex: development, regional heterogeneity, gender difference, asymmetry, intersubject variability and cortical architecture. *Hum Brain Mapp* **5:** 218–221

Zwiers MP, Van Opstal AJ, Cruysberg JR (2001) A spatial hearing deficit in early-blind humans. *J Neurosci* **21:** RC142: 141–145